Manuscript Details

Manuscript number	PROOCE_2017_188_R1
Title	Bottom trawling at Whittard Canyon: evidence for seabed modification, trawl plumes and food source heterogeneity
Article type	Full Length Article

Abstract

Fishing vessels are attracted to the dendritic Whittard Canyon system due to the abundance and diversity of species found there. Both midwater and bottom trawling are commonplace, including on deep canyon channel floors. Bottom trawling is identified here as a possible cause of changes to seafloor roughness along the canyon interfluves. An Arc Chord Ratio (ACR) rugosity index is calculated for the Whittard area and correlated with Vessel Monitoring System (VMS) data using various statistical models. Over higher slopes or rougher ground the heavily fished locations show a more homogeneous rugosity distribution than those lightly fished, indicating possible smoothing of the seabed. Bottom trawling activity on adjacent interfluves/shelf is known to generate energetic turbid, sediment plumes within the canyon branches to 2500 m depth, with elevated Suspended Particulate Matter (SPM) concentrations in the water column up to 400 m above the seabed. Lipid biomarker analysis of organic material collected from these plumes showed higher concentrations of total lipids at sites that are intensively trawled (east). In comparison to sites that are less intensively trawled (west), higher contributions of fatty alcohols were detected. While lower concentrations of unsaturated fatty acids were detected, biomarkers indicative of phytoplankton accounted for 93.4±0.7% of total lipids identified from eastern samples suggesting rapid transport of labile compounds. Results presented here suggest that intensive trawling induced changes to sediment transport will complicate the interpretation of biogeochemical property distributions at canyon systems, particularly from single surveys. Anthropogenically generated heterogeneity in sediment supply and character will also impact on habitat suitability for resident ecosystems.

Keywords	Trawling Plumes; Whittard Canyon; Suspended Particulate Matter; Vessel Monitoring System; Rugosity Index; Lipid Biomarkers
Manuscript category	Interdisciplinary

Corresponding Author	Eoghan Daly
Corresponding Author's Institution	National University of Ireland, Galway
Order of Authors	Eoghan Daly, Mark Johnson, Annette Wilson, Hans Gerritsen, Kostas Kiriakoulakis, Louise Allcock, martin white
Suggested reviewers	Alexis Khripounoff, Serge Heussner, Albert Palanques

Submission Files Included in this PDF

File Name [File Type]

Trawling_Whittard_INCISE_Responses_301117.docx [Response to Reviewers]

Highlights_301117.docx [Highlights]

Trawling_Whittard_INCISE_REVISION_291117.docx [Manuscript File]

Trawling_Whittard_INCISE_Figures_and_Tables_301117.docx [Figure]

To view all the submission files, including those not included in the PDF, click on the manuscript title on your EVISE Homepage, then click 'Download zip file'.

Bottom trawling at Whittard Canyon: evidence for seabed modification, trawl plumes and food source heterogeneity, Daly et al., Ref: PROOCE_2017_188

We are grateful for the opportunity of submitting a revised version of our manuscript for the upcoming INCISE special edition. We would like to thank the reviewers for their constructive comments and suggestions which have significantly improved the revised manuscript. In response to the major and minor review comments, we have re-written and re-structured substantial parts of the manuscript as indicated below, but with particular reference to improving figure quality, combining the different methods and drawing some more substantial conclusions to the analysis. We have addressed all comments and suggestions and we note that both reviewers have expressed concerns about the crossover between this work and that of Wilson et al., (2015a, b). This was an error in over referencing the previous work to set the new results in context, which has now been revised.

Specific responses to individual reviewers are summarised below.

Reviewer 1

We have slightly amended the title of the manuscript to add reference to each aspect of the work and hopefully retain or increase its impact. The discussion section has undergone considerable re-working based on the suggestions given.

Comments:

Line 61: Reviewer 2's suggested citation was incorporated here.

Line 69: This has been clarified by making distinction between trawl doors and other ground gear.

Line 84: Changed to: adjacent to, and within

Line 85: Now described as natural 'transport' processes, we would consider that transport via riverine input could be seen as a process in the context of a canyon system.

Lines 480 onwards: The point about fishing grounds in close proximity to very steep slopes has been added (line 519) as has the fact that not all resuspended material will be transported (line 525).

Lines 496-497: In the interest of clarity the word ‘novel’ has been dropped.

Lines 507-510: New datasets are, as yet, unprocessed and a research output is many months (or years) from completion.

Line 529 onwards: The discussion of the trawling plumes has been re-written, and in that section and throughout discussion, the importance of trawl plumes has had its emphasis increased. The intention of the comparison of the turbulent dissipation estimates (not current speeds) with non-trawl plumes was more to show that the values deduced from the basic analysis were not inappropriate for a gravity flow. The section has been re-written to take this into account.

In general, the discussion section has been rewritten to provide a more coherent and stronger set of comparisons, implications and conclusions.

Figures:

Fig 2: To reduce confusion this figure has been split in two with part (a) introducing the region’s bathymetry and areas of interest and includes depth contours. Part (b) introduces fishing effort. Many colour schemes were sampled but the original was preferred.

Fig 3: Thank you for pointing out the flaws of this figure. It has been removed and replaced. The new figure 3 shows maps of slope and rugosity for the region. It was not possible to display a VMS fishing grid overlaying slope or rugosity without confusion or colours clashing. Instead, contours of VMS fishing have been added to rugosity. Depth contours were retained with the slope map for further information.

Fig 5 (previously Fig 4): This figure stems from an initial analysis of the data and depicts the variation in rugosity (rather than rugosity itself) as it changes with increasing slope. This can be seen as a proxy for ‘heterogeneity’ of seafloor roughness. Description of this has been strengthened in the text (line 334).

Fig 7 (previously Fig 6): We appreciate that the presentation of two along channel sections could be skewed by the aliasing of the data (mostly in the near seabed data) so a new approached was used. Here the post trawling event is still shown as the intention was to highlight that the channel is filled to several 100 metres above bottom with significantly enhanced SPM concentrations. We have also included where maximum SPM concentrations

were found under natural conditions (as discussed by Wilson et al 2015) as a comparison for perspective. We have followed the suggestion to show (here selected) profiles as well to highlight the near seabed changes.

Fig 11 (previously Fig 10): While discussing benthic lifeforms and food source heterogeneity this figure is designed to aid the reader (especially non-experts) in visualising the sedimentary conditions experienced. This figure is not clamed as a result of analysis and the text (and caption) has been improved to reflect this. We would like to retain this figure.

Reviewer 2

With respect to the writing style, edits have been made to make the text more concise.

References have been added as per PDF comments.

Restructuring has taken place between sections as per PDF comments. These and further restructuring of the introduction and discussion sections provides a more defined framework to the manuscript.

With the helpful comments of both reviewers, we now realise how it could appear like we are presenting previous work carried out by Wilson et al., (2015a) again here. We have endeavoured to highlight the development of the new work/results from the old throughout the revised manuscript.

With respect to VMS data, there is a misconception that the data is a census of fishing activity rather than a statistical representation. This has now been described in detail including statistical errors in the methods section. As far as I am aware AIS data is currently only available closer to shore, within VHF radio range (10-20 nautical miles), although newer satellite systems (SAIS) are presently coming on-stream.

An appendix of GAMs mathematics has not been included, because it is incredibly difficult to glean the precise mathematics used by the models. This is due to the fact that the internal mathematics seem to be only accessible through computer code in R. Instead there is a general GAMs model equation and description added to the methods section which includes references to literature and code for any reader wishing to pursue it further.

Following are replies to specific numbered PDF comments. Any comments dealt with above or changed exactly as recommended are not included below.

Comments:

[Comments 2-4]: Text has been re-written

[Comment 10]: A sentence has not been added here about detailed calculations of global trawled area. It has been mentioned briefly in sentence one of this paragraph. At time of writing, the book Submarine Geomorphology was not available, nor do we currently have access to it, therefor we plan not to use it.

[Comment 12]: This sentence has been changed in line with suggestions from Reviewer 1

[Comment 13]: Halpern et al., (2008) has been included but Oberle et al., (2018) has not, as mentioned above

[Comments 14, 15]: Wilson et al., (2015a) did not analyse sediment dynamics (lines 125-127). Further clarifications are to follow in the writing e.g. biogeochemical analysis here is new additional analysis on the samples described in Wilson et al., (2015a)

[Comments 16-18]: Please see new writing addressing in detail the concerns over VMS data, how it was filtered and inclusion of errors

[Comment 19]: Wilson et al., (2015a) has been removed here. They essentially just named the canyon branches as WC1-4 and this work simply carries on using the same naming convention. GIS analysis carried out for this paper occurred after Wilson et al., (2015a) was published

[Comment 22]: Please note these errors quoted are for 'fishing effort (hrs)' (line 323) and are different to the errors mentioned for 'fishing records' (lines 167-169)

[Comment 23]: This has been added as part of Fig. 6 (previously Fig. 5)

[Comments 24, 25]: This paragraph has been re-written to be more descriptive and explanatory of the results of Fig 6 (previously Fig 5), however, in the interest of aesthetics, graphics were not added to the figure to point out the deflecting contours above 10 degrees.

[Comment 26]: This new figure has been added as Fig. 4 and placed before the old Fig. 4 because it came earlier in the analysis process.

[Comment 30]: lines 381-384 address the difference between Wilson et al., (2015a) and this work.

[Comments 32-34]: This section has been re-written in line with the new figure

[Comments 39-41]: This text has been moved to methods section

[Comments 42, 43]: Revised

[Comment 44]: We agree that the word typical was used too much and has been edited where appropriate. It was a reference to conditions under the natural (i.e. non-plume) driving forces that have been identified previously. That is now stated in the text.

[Comment 50]: We are unsure how to present the results of our statistical analysis as percentages.

[Comment 55]: We do not have any data for sediment sizes within Whittard and published data are referenced elsewhere in the text (Amaro et al., 2016). We have, however, re-written the sentence in question to improve on its detail.

[Comment 56]: This has been rephrased.

[Comment 57]: It is unclear as to the specifics of this comment. An effort has been made to improve the text in connection to this figure.

[Comment 61]: Text has been enhanced in this paragraph and the figure caption has been amended. Please also see response comments to reviewer 1 above, on this matter (Fig 11).

Highlights

- Evidence for seabed modification by bottom trawling activity
- Trawl plume material and associated energy dissipates down canyon channels
- Heterogeneity in down canyon organic transport varies with trawling variability
- Heterogeneity may cause complication in interpreting biogeochemical distribution

Bottom trawling at Whittard Canyon: evidence for seabed modification, trawl plumes and food source heterogeneity

Eoghan Daly[1,2], Mark P. Johnson[1], Annette M. Wilson[3], Hans D. Gerritsen[4], Konstadinos Kiriakoulakis[5], A. Louise Allcock[6] and Martin White[1,2].

1. Earth and Ocean Sciences, Ryan Institute - School of Natural Sciences, National University of Ireland, Galway, Ireland.
2. Irish Centre for Research in Applied Geoscience (ICRAG), National University of Ireland, Galway, Ireland.
3. Alfred Wegener Institute, Biologische Anstalt Helgoland, 27498 Helgoland, Germany.
4. Marine Institute, Rinville, Oranmore, Co. Galway, Ireland.
5. Natural Sciences and Psychology, Liverpool John Moores University, UK.
6. Zoology, Ryan Institute - School of Natural Sciences, National University of Ireland, Galway, Ireland.

Abstract

Fishing vessels are attracted to the dendritic Whittard Canyon system due to the abundance and diversity of species found there. Both midwater and bottom trawling are commonplace, including on deep canyon channel floors. Bottom trawling is identified here as a possible cause of changes to seafloor roughness along the canyon interfluves. An Arc Chord Ratio (ACR) rugosity index is calculated for the Whittard area and correlated with Vessel Monitoring System (VMS) data using various statistical models. Over higher slopes or rougher ground the heavily fished locations show a more homogeneous rugosity distribution than those lightly fished, indicating possible smoothing of the seabed.

Bottom trawling activity on adjacent interfluves/shelf is known to generate energetic turbid, sediment plumes within the canyon branches to 2500 m depth, with elevated Suspended Particulate Matter (SPM) concentrations in the water column up to 400 m above the seabed. Lipid biomarker analysis of organic material collected from these plumes showed higher concentrations of total lipids at sites that are intensively trawled (east). In comparison to sites that are less intensively trawled (west), higher contributions of fatty alcohols were detected. While lower concentrations of unsaturated fatty acids were detected, biomarkers indicative of phytoplankton accounted for 93.4±0.7% of total lipids identified from eastern samples suggesting rapid transport of labile compounds. Results presented here suggest that intensive

trawling induced changes to sediment transport will complicate the interpretation of biogeochemical property distributions at canyon systems, particularly from single surveys. Anthropogenically generated heterogeneity in sediment supply and character will also impact on habitat suitability for resident ecosystems.

Keywords: Trawling Plumes; Whittard Canyon; Suspended Particulate Matter; Vessel Monitoring System; Rugosity Index; Lipid Biomarkers

1. Introduction

The continental margin, occupying a little over 10% of the ocean surface area, connects the shelf seas (and hence coastal regions) to the deep sea, plays a significant role in the provision of food and energy resources, is a site for biogeochemical cycling (including carbon sequestration), and hosts a range of diverse ecosystem habitats and associated ecosystem services (e.g. Levin and Dayton, 2009; Benn et al., 2010; Levin and Sibuet, 2012). The margin is an area of heterogeneous habitat driven, in part, by the variation in continental morphology and topographic features, including slope variations, banks, mounds, seeps and canyons (Levin et al., 2010). In particular, sedimentary slopes are the most extensive margin habitat and contain the most numerous and diverse benthic communities (Grassle and Maciolek, 1997; Levin and Sibuet, 2012). There is a growing anthropogenic impact at these margin environments (e.g. Eastwood et al., 2007; Benn et al., 2010; Doney, 2010; Ramirez-Llodra et al., 2011). In particular, the spatial expansion of bottom trawling (Morato et al., 2006) into the deeper environment has been recognized as a significant element in modifying both seabed morphology and the sediment flux across the margin (e.g. Benn et al., 2010; Puig et al., 2012; Martín et al., 2014b; Oberle et al., 2016a). Both anthropogenic and natural drivers of ecosystem change at the continental margin require further quantification as a foundation for offshore resource management and conservation (e.g. Davies et al., 2007; Benn et al., 2010).

Bottom trawling covers ground area comparable to between half (Watling and Norse, 1998) and three quarters (Kaiser et al., 2002) of the world's continental shelves, can globally drive sediment flux similar in quantity to fluvial input (Oberle et al., 2016a) and can have greater impact on the seabed than all other anthropogenic pressures combined (Eastwood et al., 2007; Halpern et al., 2008; Benn et al., 2010). These impacts are exacerbated in deeper, off-shelf waters where background energy levels and species resilience is lower and habitat recovery time slower (Kaiser et al., 2002). Bottom trawling gear makes direct contact with the seafloor and is responsible for the sorting and layering of sediments, for overturning, breaking up sediment fabric and causing bed armouring (Martín et al., 2014a; Oberle et al., 2016b). The degree to which the seafloor is affected depends on bottom type, gear design and ground contact (Gerritsen et al., 2013), with trawl doors causing the most acute damage (O'Neill and Summerbell, 2011), while sweep lines, bridals and footropes cause the most widespread damage (Martín et al., 2014b). In addition to physical alterations, trawling activity can also alter the biogeochemical composition of local sediments (Pusceddu et al., 2005a, b), with compositional changes being more influential than the seasonal input of organic matter in some areas (Sañe et al., 2013). Fishing grounds commonly have lower concentrations of flocculent Organic Carbon (OC) due to winnowing and oxygenation (Martín et al., 2014a; Pusceddu et al., 2014). Given these significant changes, the resuspension of organic matter from coastal and shelf regions by bottom trawling will likely increase OC export rates to the deep (Martín et al., 2008; Palanques et al., 2014). Furthermore, heavy metals and other pollutants buried in coastal sediments can be released by trawling activity and transported to deeper more vulnerable areas (Jones, 1992; Palanques et al., 1994).

Submarine canyons provide a conduit for sediment flux between the shelf and deep ocean along the world's continental margins and, as such, both the deep sea and submarine canyons are now recognised as potential major repositories for anthropogenic wastes and marine litter, including plastics (e.g. Pham et al., 2014). There are many natural transport processes that control sediment erosion, transportation and deposition adjacent to, and within, submarine canyons, such as storm waves (Sanchez-Vidal et al., 2012), river input (Khripounoff et al., 2009), dense shelf water cascading (Canals et al., 2006) and slope failure, each dependent on local or regional physical conditions. When compared to natural canyon transport processes that drive sediment flux, several studies have discussed anthropogenic impact, through bottom trawling, as a major, if not dominant, process, especially on human time scales (e.g. Halpern et al., 2008; Puig et al., 2012; Martín et al., 2014b; Puig et al., 2014). Additionally,

bottom trawling in proximity to submarine canyons has been found to smooth out the seascape on large spatial scales, for example, at La Fonera Canyon (Puig et al., 2012; Martín et al., 2014a; Martín et al., 2014c; Payo-Payo et al., 2017), where changes to topography are now clearly visible on high resolution bathymetry maps (Puig et al., 2012). Trawler induced sediment gravity flows in La Fonera Canyon have been described in detail by Martín et al. (2014c). Payo-Payo et al. (2017) highlighted, through modelling anthropogenic sediment resuspension/transport, the ability of bottom trawling to affect wider areas than the fishing grounds, contrasting localised resettling on-shelf and over canyon flanks with widespread and distal displacement from sediment turbidity currents, especially over the steeper slopes.

Changes to morphology and biogeochemistry caused by bottom trawling in submarine canyons can affect ecosystem functioning and massively reduce benthic habitat heterogeneity (Watling and Norse, 1998; Puig et al., 2012 and references within). Trawling of the seafloor, negatively impacts on the biodiversity and abundance of life found there (Watling and Norse, 1998; Puig et al., 2012; Pusceddu et al., 2014); greatly reducing infaunal communities (O'Neill and Summerbell, 2011) when compared to untrawled areas.

In this paper the potential impacts of fishing on seabed morphology and down-canyon sediment distribution and associated biogeochemical parameters at the Whittard Canyon system on the Celtic Sea margin, NE Atlantic (Fig.1) have been assessed. The Whittard Canyon is a dendritic system with canyon heads cutting the shelf at 180–200 m and a main channel axis opening onto deep ocean floor at 3600–4400 m (Reid and Hamilton, 1990; Amaro et al., 2016). Whittard Canyon has limited sediment input from fluvial processes due to its distance (~ 300 km) from land, but does experience significant off-shelf material flux. This is due to high overlying pelagic productivity (Sharples et al., 2013) and dynamical processes such as boundary currents and internal waves which drive transport via nepheloid layers (Wilson 2015b; Hall et al., 2017), slope failure and sediment gravity flows (Amaro et al., 2016). Additionally, Wilson et al. (2015a) observed Enhanced bottom Nepheloid Layers (ENLs) with significantly higher sediment concentrations in two branches of Whittard Canyon. These ENLs were correlated with fishing activity, via Vessel Monitoring System (VMS) data, to determine their anthropogenic origin but no detailed analysis of the plume dynamics were made at that time.

[**Figure 1** here please, at 1.5 columns wide]

Results are presented here in two parts; (i) a statistical comparison of fishing intensity and seafloor rugosity is carried out through a generalized additive model (GAM) fit, and (ii) a brief assessment is made of the dynamical and biogeochemical characteristics of the resulting trawl-induced sediment plumes found in the Whittard Canyon branches. Results are discussed with respect to potential issues in interpretation of suspended sediment distribution patterns, biogeochemical signatures and potential impacts on ecosystem functioning within this and similar canyon systems.

2. Methods

2.1. Spatially distributed fishing intensity and seafloor roughness

Vessel Monitoring Systems (VMS) are used internationally for tracking vessel activity including fishing vessels. In the Whittard region, the fishing activity consists of northern and southern European fishing fleets. The spatial distribution of fishing fleets can change due to factors such as targeting different specific species or the cost of fuel (Gerritsen and Lordan, 2011). VMS monitoring is administered within the Irish Exclusive Economic Zone (EEZ) by the Irish Navel Service. Speed and position data are sent via satellite from each vessel at a minimum frequency of once every two hours. VMS data for this study were extracted for the period from January 2006 to February 2016 and then linked to logbook data to identify the gear type used (following methods described by Gerritsen and Lordan, 2011). Only bottom trawling vessels (which directly affect the seafloor) were retained in the dataset. Gear types used were bottom otter trawls (OTB), bottom pair trawls (PTB) and otter twin trawls (OTT) (Nédélec and Prado, 1990). Fishing effort was defined according to Gerritsen and Lordan (2011). Each VMS record was assigned an effort value that was equal to the time interval since the previous record (generally 2 h). Records with time intervals > 4 h were given an effort value of 4 h. The data were then filtered to exclude vessel speeds < 0.5 knots or > 4.5 knots in order to retain only the records that correspond to fishing activity. VMS data were then gridded to their provided resolution of 0.01 x 0.01 decimal degrees, or 740 m (east/west) x 1110 m (north/south) at these latitudes, for analysis using Geographical Information System (GIS) applications (Fig. 2b). It might be expected that the size of the grid cells should be

approximately equal to the distance that a vessel can travel between successive VMS records, otherwise the vessel could travel over a number of grid cells without being recorded, leading to bias. However, this is not the case. Instead, each VMS record is a *sample* of a vessel's location (a systematic sample over time) and the number of VMS observations in each grid cell will therefore be proportional to the amount of time the vessels have spent in that cell. The resolution of the spatial grid is therefore not limited by the distance that a vessel can travel between successive VMS records, but instead by the number of records in each grid cell. Because the data are essentially count data, the precision can be estimated using a Poisson distribution. At the current resolution, 95% of grid cells in the study area had at least 10 VMS records (relative standard error: 32%) and the mean number of records was 47 (relative standard error: 15%).

[**Figure 2** here please, at 1.5 columns wide]

Bathymetry was obtained from the Irish National Seabed Survey (INSS) for the Whittard Canyon region (extent: 48.416 to 49.105 N; −11.505 to −9.846 E). The INSS was carried out between 1999 and 2005, covering the majority of the Irish marine continental area and is freely accessible through the Geological Survey of Ireland (GSI) at a resolution of 0.001 x 0.001 degrees (~ 74 m by 111 m). Rugosity, a non-standardised (unitless) descriptor for seafloor roughness, was extracted using bathymetry data, point averaged down to VMS grid resolution and then analysed for correlations with VMS fishing effort. Here an Arc-Chord Ratio (ACR) rugosity index was derived through a dedicated toolbox developed by Du Preez (2012) on an ArcGIS platform. The advantage of an ACR rugosity index is that it decouples background slope from the rugosity determination using a plane of best fit, rather than a more traditional horizontal plane. It is scale independent, therefore, making it well suited for use over the complex topographical features found around the Whittard Canyon.

Individual canyon branch polygons were drawn up within the canyon system to further scrutinise variation in fishing and potential sediment remobilisation across each location. These polygons (Labelled: WC1–WC4 in Fig. 2a) were delineated using depth contours and distance from canyon branch channels. The deep ends of the canyon branch polygons were bound to the 2000 m depth contour. The polygons' sides make a line orthogonal to depth contours where the contours turn most sharply, stepping down from the canyon interfluves. The upper end of the polygons (where not touching another polygon) are defined to be a VMS grid cell above or touching the 200 m contour, in order to include those VMS cells as part of that canyon branch

analysis. Although this approach is somewhat subjective, it is a best attempt at placing boundaries between these complexly shaped spurs and channels. Further polygons were drawn within these canyon branch divisions in an effort to focus on trawled areas that have the largest effect on sediment transport into the canyon channels. One approach here was to alter the original polygons by using a 10 hour VMS fishing contour as the inner or channel-side boundary, in order to isolate, for analysis, the regularly fished interfluves of the original polygon from the canyon axis. A second approach was to identify areas at the steepest limits of fishing occurrence over slopes with greatest potential for down canyon sediment supply; these strips are approximately 500 m wide and situated directly above areas of > 20° slope. Fishing rarely occurred anywhere steeper than a 20° slope angle (Fig. 3a).

Potential influences on the rugosity of the seabed were considered to be broad scale geographic gradients, slope and fishing intensity. Estimates of the contributions of these variables were made using generalized additive models (GAMs). An example of a GAM in general form is as follows:

$$\mu_i \equiv E(R_i); \quad g(\mu_i) = X_i\beta + S_1(x_{1i}) + S_2(x_{2i}, x_{3i}) + Ln_i S_3(x_4) + \ldots \qquad (1)$$

Where μ_i is the expected value of the response variable R_i and g is a known, monotonic, link function; $X_i\beta$ represents any fully parametric components of the linear predictor while $S_{1i,2i,3i\ldots}$ are the smooth functions of the predictor variables ($x_{1i,2i,3i\ldots}$); Ln_i is included here as an example linear functional of s_{3i}, where there can be multiple or no such linear functional terms throughout the model (Wood and Augustin, 2002; Wood, 2006; Wood, 2017). R_i here is the interpolated rugosity value for each fished VMS grid cell. Predictors ($x_{1i\text{-}4i}$) were the latitude and longitude of each grid square (for geographic patterns), the estimated slope and the total fishing hours. GAMs were used because they provide a flexible statistical modelling framework for investigation of potentially nonlinear relationships, including interactions between predictor variables. Fitted GAMs are smoothed functions through the data using penalised regression splines, such that for example:

$$S(x) = \Sigma_{i=1} f_i(x)\beta_i \qquad (2)$$

Where the smooth function S constitutes values for the unknown parameters β_i and where f_i are chosen and known 'basis functions' on which the smoothing formulae rely on (Wood, 2006; Wood, 2017).

Screening of the data suggested that the data were not normally distributed. GAMs were therefore estimated (in R package mgcv, Wood, 2017) using a log-link to reflect the log-normal response variable. A number of models are possible given the four predictor variables investigated. The comparisons of interest were defined as a purely geographic pattern (predictors: latitude and longitude), a model based on just slope and fishing hours, and models where variables were allowed to interact in pairs or with all four variables together. Interaction terms test the hypothesis that the relationship of the response variable to a predictor is not fixed, but depends on a further predictor or predictors. The most informative of the alternative models was selected using the generalized cross validation (GCV) score, with low values indicating the best model (Wood, 2017). GCV scores penalize additional degrees of freedom, so the most complex model is not necessarily chosen as the most informative.

[**Figure 3** here please, at 1 column wide]

2.2. Hydrographic Observations

Four branches of the Whittard Canyon were surveyed during summer 2013 (CE13008: 9–17th June 2013) & 2016 (CE16006: 29th May–15th June 2016) on the *RV Celtic Explorer*. Suspended Particulate Matter (SPM) was estimated from transmissometer measurements (C-star, WET labs; 0.25 m path length, operating at 650 nm) in conjunction with hydrographic measurements made with a CTD (Seabird SBE 911) and SBE32 rosette. Raw values (volts) were converted to SPM (µg l^{-1}) following the linear regression of beam attenuation values and the mass of SPM obtained from filtered water samples (Wilson et al., 2015b).

An assessment of the dynamical characteristics of recent trawling plumes measured was made using vertical CTD profiles. The turbulent length scales and first order estimation of magnitude in turbulent kinetic energy dissipation were quantified through Thorpe Length scale (L_T) analysis (Thorpe, 1977; Dillon, 1982). This method estimates the characteristic length scale (L_T) of density overturns within a CTD profile of sufficient vertical resolution (here 0.25m CTD data was used). L_T is determined by reordering a profile of individual density values (ρ_i at depth z_i) into one where density increases monotonically with depth (ρ_i at depth z_o). A corresponding profile of density displacements ($z_i - z_o$) is produced. L_T is then defined as the RMS displacement value over an appropriate averaging process. This averaging is typically over individual overturns in a 'packet' of finite vertical extent where

the sum of the individual Thorpe displacements equals zero, and that are not associated with instrument noise (e.g. Galbraith and Kelley, 1996; Mater et al., 2013). Furthermore, a simple estimate of the energy dissipation (ε) can be made following the arguments of Dillon (1982) and assuming L_T is proportional to the Ozmidov length scale, Lo, which is used to describe the scale of turbulence in a stably stratified flow. Here we note caution in that L_T is principally a method to estimate the vertical eddy size from the density profiles and only a limited method to fully quantify the turbulence (e.g. Mater et al., 2013).

Assuming that L_T and L_O are proportional, ε can be found from a measurement of L_T,

$$\varepsilon = 0.64 * L_T^2 * N^{-3} \quad (3)$$

where N is the buoyancy frequency ($N^2 = [-g/\rho_0] * d\rho/dz$).

2.3. Biogeochemical analysis of suspended particulate material

Suspended particulate organic matter (sPOM) was collected using a Stand Alone Pump System (SAPS; Challenger Oceanic), deployed by a winch on the CTD wire or attached to the CTD. Large volumes of water (163–1143 l) were filtered through two stacked pre-combusted (400 °C; > 6 hrs) glass fibre GF/F (Whatman, 293 mm diameter) filters at the surface and near bottom depths (7–22 m above the seabed). Filters were folded into quarters, wrapped in pre-combusted aluminium foil on recovery and stored at −80 °C for the duration of the cruise. Filters were subsequently freeze-dried and stored at −20 °C until analysis.

Elemental and molecular analysis was carried out on sPOM collected from Bottom Nepheloid Layers (BNLs) between 1310–1370 m water depth (< 20 m above the seabed) from the four branches and a surface sample (locations: Fig. 2a). Particulate organic carbon (POC) and particulate nitrogen (PN) were measured from punched circles (113 mm^2) in homogeneous areas at the middle and edge of the top filter only. Analyses were carried out using a CEInstruments NC 2500 CHN analyser in duplicates and the mean value was taken. POC values were obtained after de-carbonation of the filters (HCl vapour method; Yamamuro and Kayanne, 1995), whereas PN values were determined without de-carbonation. Mean values of the middle and edge filter samples were taken to eliminate filtration artefacts. Concentrations below the limit of detection (< 0.01) were considered nil. Values were not

corrected for dissolved organic material due to the large volumes of water filtered (Moran et al., 1999).

Lipid extractions and analyses of suspended Particulate Organic Matter (sPOM) were carried out according to the methods of Kiriakoulakis et al. (2007; 2009; 2011) to determine the total fatty acid and alcohol content. Briefly, portions (1/4) of the SAPS filter (~ 6.21–7.75 g) were spiked with 20 µl of internal standard (100 ng/µl 5α(H)-Cholestane; Sigma) and extracted by sonication (30 min @ 30 °C; x 3) in ~ 20 ml dichloromethane:methanol (9:1). Extracts were later transmethylated (24 hrs; 40 °C) with 1 ml methanolic acetyl chloride (30:1) and derivatised with 50 µl of *bis*-trimethylsilyltrifluoroacetamide (BSFTA, 1% trimethylsilylchloride; Stigma; 30 min @ 40 °C). Extracts were stored at −20 °C until analysis.

GC-MS analysis was carried out using a Varian 450 Gas Chromatographer Mass Spectrometer. Extracts were run in batches and loaded onto the column (Agilent VF-MS column: 30 m x 0.25 mm, 0.25 µm; carrier gas helium @ 1 mL min^{-1}) using a CP8400 autosampler and a CP-1177 split/splitless injector. The column was fed directly into the electron (EI) source of a Saturn 220 mass spectrometer (ionisation potential 70 eV; source temperature 220 °C; trap current 300 µA; full data acquisition mode). Chromatograms were reviewed and processed using Varian MS Workstation software (version 6.9.1). Compounds were identified by comparison of their mass spectra and relative retention times with authentic standards (Supelco TM37 FAME mix; 47085-U; 47015-U; 47033 Sigma-Aldrich) using the total ion current (TIC) chromatogram. Compound concentrations were calculated by comparison of peak areas of the internal standard with those of the compounds of interest. The relative response factors of the analytes were determined individually and/or for similar compounds. Organic contamination in procedural blanks extracted with each sample batch was subtracted from the sample values. Reproducibility of similar lipid analyses was determined to be $\pm$ 15% by Kiriakoulakis et al. (2000). Concentrations were normalised to volume of water as an indicator of food availability. The contribution of phytoplankton in each sample was calculated by the sum of C_{14} – C_{22} saturated fatty alcohols (Volkman et al., 1998), straight chained fatty acids and $C_{16:1(n-7)}$ (Harwood and Russell, 1984; Conte et al., 2003) and PUFAs (e.g. Duineveld et al., 2012); see also supplementary information. Similarly, bacterial indices were calculated by the sum of $C_{18:1n7}$ and odd numbered saturated and branched fatty acids (Volkman and Johns, 1977; Duineveld et al., 2012).

3. Results

3.1. Bottom trawling intensity and rugosity correlation

Fishing occurred up to depths of around 1300 m right across the region studied (~ 7744 km^2), with fishing intensity clearly related to bathymetry and to large scale canyon features, such as interfluves or plateaux, up as far as the shelf break (Fig. 2b). The combined total time spent by the fishing industry engaging in bottom trawling was 1.46 x 10^5 hours or just under 17 years over the 10-year period analysed. Over each VMS grid square (approximately 0.82 km^2) actively fished in the 10 years, the mean fishing effort was 4.8 hrs, median fishing effort was 23.4 hrs and the highest fished grid-square saw 208 hrs of bottom trawling (fishing effort from VMS having an accuracy of approximately 88% after Gerritsen and Lordan, 2011). The highest bottom fishing values were found out along the interfluves and plateaus adjacent to steeper slopes. Although concentrated on lower slopes and shallower waters, fishing effort regularly occurred on steeper inclines (> 10°) on canyon flanks around the edges of interfluves and occasionally in waters deeper than 1000 m. As of December 2016, deep-sea bottom trawling below 800 m deep is prohibited in these waters by EU law (EU 2016/2336).

[**Figure 4** here please, at 1 column wide]

In an effort to assess the most appropriate type of analysis, an initial plot of rugosity against slope was constructed with fishing points split between high and low around their median (Fig. 4). This identified the non-linear nature of the dataset, where the relationship between slope and rugosity may be different with different levels of fishing activity. High levels of fishing only occurred on low slopes and less complex rugosity, whereas low levels of fishing occurred over the whole region considered. Further examination of the data suggested that the calculated variation in rugosity among grid squares was lower in more heavily fished areas. This pattern changed with slope (Fig. 5). By splitting the rugosity values into heavily and lightly fished grid squares (using median fishing effort: 23.4 hrs), standard deviation of rugosity can be summarized for each subset, and viewed as a proxy for heterogeneity of seafloor roughness. For shallower slopes there was no difference between high and low

fished grid squares, but at higher slopes the more heavily fished areas had less variation in rugosity (roughness) values.

[**Figure 5** here please, at 1 column wide, with black and white for print and colour for online viewing]

There was statistical evidence for location, slope and fishing intensity all being related to changes in rugosity (Table 1). Judged by GCV scores, models with only two variables were inferior to a model that contained all four predictors (comparing models 1–3). Allowing all four variables to interact (model 4) did not improve predictive value compared to the model where all variables had independent effects (model 3). A model with terms where slope and fishing interacted, along with a geographic interaction (model 6), had the lowest GCV score and highest adjusted-R^2 of the alternative models. This can therefore be viewed as the most informative summary of the relationships between variables.

[**Table 1** here please]

The geographic effect (Fig. 6a) is a general decrease in rugosity with increasing latitude, with some variation in the rate of change with longitude, as is expected in this area going from deep canyon to shelf. Independent of the geographic pattern, rugosity contours show increasing roughness with steeper slopes (Fig. 6b). The interaction with fishing intensity indicated a local increase in rugosity for low slope areas (particularly between 30 and 100 fishing hours), reflected in the deflection of the fitted contour at low slopes. For example, the average rugosity on seabed with less than 0.5 degree slope was 1.0048 (SE 0.00011) between 40 and 70 VMS hours and 1.0045 (SE 0.00011) at all other VMS values. Rugosity contours for areas with slopes steeper than 10° suggested that rugosity decreased with increased fishing. This pattern can be interpreted by comparing areas with low and high fishing effort for the same slope value. For example, at zero fishing, the predicted residual variation rugosity is above 0.005 on a 10° slope; at 50 fishing hours residual rugosity was predicted to be below 0.005 at the same slope value.

[**Figure 6** here please, at 1 column wide]

An east-west variation in fishing intensity was discovered across the four main canyon branches studied (WC1–WC4). Due to its geometry and the distribution of fishing intensity around that channel, WC4 was the largest probable contributor to down-slope sediment flux;

followed by WC3 (Table 2). WC2 and WC1 to the west contributed least. By focussing on the interfluves flanking the WC4 canyon branch channel, the largest fishing intensity per area (79.6 hrs km^{-2} over the 10 years) was identified out of the whole region. There was very little fishing occurring on slopes greater than 20°, consequently this was chosen as a boundary between slopes fished and not fished. As with individual canyon branch results, these focused areas (Table 2), such as ones fished just above slopes of 20°, displayed a steady west to east increase (~ 5.3 hrs km^{-2}) in fishing intensity.

[**Table 2** here please]

3.2. Sediment plumes within the canyon channels.

Trawling, whilst modifying the seabed, also generated sources of suspended material at the shelf edge adjacent to the branches of the Whittard system. Sediment plumes had been observed in branches WC3 and WC4 during the 2013 survey (Wilson et al., 2015a). Since those reported observations, further plumes have been observed in the WC2 and WC4 branches during a subsequent survey in 2016. Both the along canyon and mid-water conditions due to trawling plume activity were apparent from vertical profiles of 10m averaged derived SPM concentrations (Fig. 7). Under what were considered typical conditions (i.e. no trawling plumes evident), Benthic Nepheloid Layers (BNLs) of thickness 100–200 m have SPM concentrations within a canyon branch similar to that of corresponding surface plankton layers (0.15–0.4 mg l^{-1}, hatched shading in Fig. 7a). The highest values occurred at bottom depths associated with boundary currents or internal wave energy enhancement (Wilson, 2015b). The immediate aftermath of what was considered a trawling plume event in WC4 resulted in an increase in benthic layer SPM concentrations, in excess of 1 mg l^{-1}, throughout the entire length of the canyon branch that was sampled (Fig. 7b). Maximum BNL SPM concentration was 8 mg l^{-1} within the mid-canyon section. Furthermore, values in excess of 0.3 mg l^{-1}, found over small spatial extents at certain depths in normal conditions, now occupied the lower 200–400 m adjacent to the seabed along the entire >45 km of the canyon branch surveyed.

[**Figure 7** here please, at 1.5 columns wide]

Under non-trawling plume conditions, individual vertical profiles of density and derived SPM showed a bottom boundary layer region from 1300 m to 15 mab (metres above seabed) marked by a step in the density gradient (Fig. 8a). No well-defined bottom mixed density

layer was apparent in the profile shown in Fig. 8a, although often present in other vertical density profiles. An overall stratified layer up to 600 m depth was present above the bottom layer, associated with the depth range at, or adjacent to, the permanent thermocline (Fig. 8a). The mid water layers contained small vertically homogeneous/near homogeneous density layers, including reversals in the density gradient, of vertical extent 1–10 m. A BNL in the lower 50 m of the water column is associated with a peak value of SPM reaching 1 mg l^{-1} (Fig. 8b). A subsequent vertical profile made five days later at the same location indicated a much more turbid BNL with a peak value of 7.7 mg l^{-1} (the axis scale truncates the plume), but with a significant increase in background (mid water) SPM concentrations from ~ 1200 m depth, or ~ 170 mab. This high concentration BNL was associated with a well-mixed bottom density layer capped by a pycnocline of density difference ~0.05 kg m^{-3} (Fig. 8f).

Associated with the vertical profiles of density and SPM, individual Thorpe density displacements in mid water occurred with magnitude up to 1–5 m over small vertical extents, with an increase in the magnitude of displacement packets below 1000 m (Fig. 8c). A large overturn was highlighted between 1200–1300 m, with maximum displacements peaking at 30 m immediately above the bottom boundary region. For the plume event, similar mid water characteristics in Thorpe displacements were again present but with a significant increase in amplitude per overturn region below 1150 m. Increased amplitude in displacements (up to 20 m) between 1200–1300 m were associated with the upper of the two-layer BNL and maximum displacements immediately above the seabed. L_T values up to 2 m were found between depths 600–1000 m, with values increasing to ~ 5 m below 1000 m and a peak of 12 m associated with the upper layer of the BNL (Fig. 8d). Corresponding values of the turbulent kinetic energy dissipation (ε) indicated that the small mid water overturns had values of ε between 10^{-9}–10^{-8} W kg^{-1} for the typical (pre-plume) scenario (Fig. 8e). The large overturn immediately above the BBL/BNL was slightly larger (3 x 10^{-8} W kg^{-1}). For the plume event, L_T values above the BNL were similar to values for a non-plume scenario, but increased significantly below 1200 m with values of O(10m) in the upper BNL and peaking at 22 m in the lower BNL layer (Fig. 8i). Turbulent energy dissipation during the plume event was generally larger in mid water compared to mid water conditions with no trawl plume present, with a number of values in excess of 10^{-8} W kg^{-1} (Fig. 8j). Values peaked between 1200–1300 m in the upper BNL with ε ~ 10^{-7} W kg^{-1}).

[**Figure 8** here please, at 2 columns wide]

A second example of a trawling plume (from the 2013 survey), showed a plume that occurred at a depth above the BBL, presumably the plume reaching equilibrium density before the seabed was reached (Fig. 9). This profile was made 30 hours after one in the same location which indicated no enhanced BNL concentration layer, and suggested a plume was captured by the CTD profile near the end of the plume event. The main plume was centred at 1200 m (water depth was 1370 m), about 100 m thick, with SPM concentration peaking at 5 mg l^{-1}, over an order of magnitude larger than non-plume BNL values (Fig. 9b). Individual overturns and displacements were fewer in number than in the previous example but generally larger in scale (30–40 m in vertical extent with displacements peaking at 15–20 m (e.g. at 850–900 m and 800 m, Fig. 9c). The upper boundary of the main plume was associated with a larger overturn between 1150–1220 m and displacements up to 30 m. Turbulent energy dissipation (Fig. 9e) was elevated for the overturns at 800, 850–900 m and for the smaller of the two plumes at 1000–1100 m, with values close to 10^{-7} W kg^{-1}, or an order of magnitude larger than the typical mid water values associated with small overturns. The main plume overturn had a value of $\varepsilon = 10^{-6}$ W kg^{-1}, the maximum energy dissipation estimated from the profiles analysed and perhaps reflecting the capture, rather than the aftermath of, the plume event.

[**Figure 9** here please, at 2 columns wide]

3.3. Variation in quality and quantity of suspended particulate material

The SAPs sampled SPM concentrations in the four E/BNLs (1308–1370 m) varied across the four branches (WC1–WC4; see location in Fig. 2a) with mean values of SPM = 1.01 ±0.86 mg l^{-1} (Table 3). Highest values were detected in WC4 (2.160 mg l^{-1}) and associated with bottom trawling activity. Although sampled during the same period of trawl activity, lower SPM concentrations (0.29 mg l^{-1}) were detected in the adjacent branch (WC3). High SPM concentrations were also detected in WC1 (SPM = 1.18 mg l^{-1}) but were not previously linked to bottom trawling on the western side of the canyon system. Material from the near-surface has a molar C/N value of 6.4, typical of oceanic surface water, while C/N values from the E/BNLs at depth ranged from 8.2–22.2 across the four branches, with the lowest values in WC4 and highest in WC1.

Lipids (total fatty acids and alcohols) detected in suspended Particulate Organic Matter (sPOM) across the four branches displayed complexity and heterogeneity in both their

composition and concentration (Fig. 10 & Table 3). As four of the five filters were torn on recovery (a sampling artefact) and POC may have passed through onto the second filter, concentrations are normalised to volume of water filter (ng l^{-1}) here rather than OC content for a more reliable interpretation. The number of individual compounds identified differed greatly, with material from the east showing less complexity (16±6 V 34±17 individual compounds). Total lipid concentrations across the four branches, ranged between 181.5–1301.9 ng l^{-1} (Fig. 10), with higher values found on the eastern side of the system. As a reference point, the concentration of total lipids in the near surface was 1510.4 ng l^{-1}, comparable to those in the east (1092.3 ±296.4 ng l^{-1}), while concentrations in the west were twice as low (349.3 ±237.3 ng l^{-1}).

[**Table 3** here please]

Variability in the principal lipid classes (saturated fatty acids, MUFAs, PUFAs and fatty alcohols) was evident (Fig. 10). Fatty acids ranged from C14 to C22 (see supplementary information for most commonly identified compounds). Saturated fatty acids and MUFAs were well represented across the four samples and accounted for 34.8 ±12.0% and 34.6 ±22.6%. PUFAs represented < 16.9%, except in the surface (36.8%). The greatest variance in dominant lipid class was observed in the alcohols, ranging from 1.8–50.8% with a mean of 3.4 ±2.3% in the western (WC1 & 2) and 46.5 ±6.1% in eastern branches (WC3 & 4).

Although PUFAs were rare, particularly in eastern branches, lipid biomarkers of phytoplankton origin accounted for 93.43 ±0.7% of the total lipids in WC3 and WC4. In comparison WC1 & WC2 had lower concentrations with 68.12 ±9.9% of the total lipids represented by compounds that indicated phytoplankton origin. Near-surface waters showed lower percentages of phytoplankton markers than any of the samples at depth (78.3%).

All samples showed some level of bacterial reworking in the lipid signatures (4.4 ±2.6%). Bacterial biomarkers followed the opposite pattern to the phytoplankton markers, with higher mean values in the western branches (6.4 ±1.9) and lower in the eastern (2.5 ±1.3%), further indicating that material in the eastern branches is more recently suspended/transported and fresher.

[**Figure 10** here please, at 1.5 columns wide]

4. Discussion

Based on a contemporary snapshot (last 10 years) of an area where fishermen have pushed out into deeper fishing grounds, fishing intensity was found to be variable across the Whittard Canyon (Fig. 2). Highest fishing intensity was generally associated with smoother morphology, especially over steeper sloping parts of canyon interfluves (Fig. 3). The trawling vessels used were only limited by the physical constraints of their gear and slopes greater than 15° (> 1300 hrs in 10 years) were regularly fished, but rarely over slopes > 20° (90 hrs in 10 years). Trawling along the continental margin immediately to the east of Whittard Canyon is seasonal, with most fishing occurring between July and March with a maximum in August (Sharples et al., 2013). Due to the considerable width of the Celtic Shelf and large distances from the nearest fishing ports, and to the size and complexity of the Whittard Canyon, the canyon does not endure the same localised fishing intensity or working weekday cycles found at other submarine canyons more connected to coastal regions, e.g. along the NW Mediterranean shelf edge (e.g. Palanques et al., 2006).

It can be estimated that grounds at Whittard are fished an average of 1.7 times per year by isolating the grounds most frequently fished as those above 800 m (an area of 4456 km^2). This value was derived from a fishing effort of 1.37 $x10^4$ hrs per year, a trawl speed of 5.5 km hr^{-1} (Pilskaln et al., 1998; O'Neill and Summerbell, 2011) and a typical door spread of 100 m for deep water fishing (Gerritsen et al., 2013; Payo-Payo et al., 2017). Assuming a re-suspended mass of 1.6 kg m^{-2} of fished area (Oberle et al., 2016), a first order estimate of 7.13 Mt total sediment per year may be mobilised and potentially available to enter the Whittard system via trawling. Notwithstanding the approximations and assumptions made here, this estimate highlights the ability for anthropogenic forcing to alter natural sediment flux, especially in areas in proximity to steep slopes with potential for triggering sediment gravity flows (Palanques et al., 2006; Martín et al., 2014c). Focusing on individual branches, ground over the flanks of WC4 were found to be fished 2.6 times the regional average, affording it the greatest potential for remobilising substrate. Using fishing intensity (Table 2), an approximation of re-suspended sediment at WC4 can be estimated (this time for 'fishing intensity', after O'Neill and Summerbell (2011), as opposed to 'fished area') of 9.54 x 10^5 tonne yr^{-1}. Even if a large proportion of this suspended material resettles locally there remains

the potential for large quantities of material to be transported down canyon to deeper waters. These rough estimates and to a lesser extent those for WC3 and WC1 & 2 further west, have implications for generation of sediment gravity flows (Martín et al., 2014a), ENLs (Wilson et al., 2015a), as well as a changing seafloor geomorphology. Traditional studies of sediment flux across continental margins must take these anthropogenic affects into consideration, especially in canyons, such as Whittard, which are more prone to a net export flux of pelagically derived organic material, (natural or anthropogenic), due to large distance from riverine sources (Oberle et al., 2016).

Our results provide a statistical interpretation of the relationship between bottom trawling and seafloor roughness in the vicinity of a large terrestrially distant submarine canyon system, using a rugosity index independent of slope. Rugosity varies across many scales and in doing so moderates benthic habitat at similar scales (Wilson et al., 2007; Dunn and Halpin, 2009). As with slope angle (20°), rugosity is a physical constraint to bottom trawling but it has proven challenging to constrain a rugosity cut-off point for fishing activity. The Whittard Canyon area is likely enduring the same effects from seafloor ploughing as those found at La Fonera Canyon in the NW Mediterranean by Puig et al. (2012) albeit at a slower rate and wider geographical area. The GAMs analysis highlighted a complex association between VMS fishing effort and rugosity (Table 1 & Fig. 6b). Where fishing activity occurred on steeper slopes, there were areas of less complex rugosity than would be expected in the absence of fishing. A cause and effect relationship, i.e. whether fishing vessels seek out sloping areas of lower complexity or whether the activity of fishing has reduced complexity in slope areas where active, could not be established. Results here, however, are in line with other studies (e.g. Puig et al., 2012; Payo-Payo et al., 2017). In this respect, future work is planned to focus on cause of seabed alteration in Whittard by conducting a 'before and after' analysis of previous (Irish National Seabed Survey, INSS) and new multibeam bathymetric surveys and correlating those results with VMS data.

Significant trawling induced sediment plumes are generated within the canyon channels of the Whittard system, remnants of which have been observed in light transmission profiles of up to 200 m thick adjacent to the seabed (Fig. 7). Such anthropogenic sourced sediment plumes had been suggested to occur in Whittard Canyon previously (Wilson et al., 2015a), and there is undisputed evidence for them in a number of canyons at the NW Mediterranean continental margin (e.g. La Fonera Canyon (Martín et al., 2014b)). Trawling induced plumes are,

therefore, another mechanism for creating down canyon sediment flows to add to those generated by naturally occurring processes, such as storm wave mobilisation of sediment (Xu et al., 2004), tidally generated (Lee et al., 2009), or riverine flood events (Khripounoff et al., 2009). The intensity and prolonged seasonal timeframe of fishing activity, however, implies that the anthropogenically generated plumes will provide a significant contribution to the integrated export flux at continental margin sites.

The sediment gravity flows observed here are energetic, with an estimated turbulent energy dissipation (ε) an order of magnitude greater than for benthic nepheloid layers that occur under background conditions, despite the observations being made post event (Figs. 8, 9). Values in ε up to 10^{-6} W kg^{-1} were estimated from Thorpe length scale analysis of density overturns in CTD profiles. The use of Thorpe length scale is a simple and indirect method to determine ε (e.g. Mater et al., 2013), with additional errors in absolute values related to the small number of overturns sampled here (e.g. MacDonald et al., 2013). Furthermore, ε is dependent on the variability of L_T with Ozmidov length scale Lo, and L_T probably represents the turbulent kinetic energy level more than the dissipation (Mater et al., 2015); also mean values should be treated with caution. Notwithstanding this, the dissipation values of ε appear reasonable in magnitude even if estimated from a few profiles. The dissipation values found here are comparable to those estimated from similar analysis, although through different forcing conditions. For example, in Gaoping Canyon a value of order 10^{-8} W kg^{-1} (Lee et al., 2009) was found using the Thorpe displacement method, ~ 2 x 10^{-6} W kg^{-1} with maximum Thorpe displacements of 30 m. In the head of Monterey Canyon Gregg et al. (2005), correcting previous values found in upper Monterey canyon using microstructure measurements (Carter and Gregg, 2002), estimated values of ε ~1.97 x 10^{-7} W kg^{-1}, but attributed this to tidal mixing.

The values found, however, do suggest the fact that the plume events were associated with enhanced turbulent kinetic energy, and keep material in suspension for extended periods of time. This was observed in the aftermath of a trawl event in WC4, with enhanced SPM concentrations apparent over a large vertical range throughout the canyon section (e.g. Fig. 7). The increase in overturn scale and dissipation values in mid water also highlight the possibility that intermediate nepheloid layers may be generated as remobilised sediment enters the channel from the interfluves where trawling is most intense (Fig. 2b). The elevated dynamics associated with such gravity flows will also allow detachment of sediment laden

water from the main plumes away from the bottom boundary, such as those observed in La Fonera Canyon at a bottom depth of ~ 600 m (Martín et al., 2014c). Evidence for that in Whittard comes from the observation of a turbid layer immediately above the bottom boundary and generally elevated turbulent energy in mid water during the event highlighted in Fig. 8. Trawl induced plumes measured in 2013 in WC3 and WC4 were found in water depths associated with the mid canyon reaches that had steepest canyon walls, which would promote gravity flows from the adjacent interfluves (Wilson et al., 2015a). The generation of thick BNLs and INLs, together with elevated turbulent energy levels within the water column, suggests that material will be kept in suspension for longer and that interpretation of BNL/INL sources, drivers and distribution patterns are likely to be anthropogenically influenced.

The impacts of potentially introducing even a small fraction of the 7.13 Mt sediment per year, suspended by bottom trawling activities into the canyon system cannot be overlooked. The area of the northern Bay of Biscay has high primary productivity, in the region of 200 gC m^{-2} yr^{-1} (Wollast and Chou, 2001). Organic carbon burial has been estimated at 0.05 g m^{-2} yr^{-1} at the upper slope break of the Goban Spur and 0.11 g m^{-2} yr^{-1} further down slope (van Weering et al., 1998). Perhaps, the high energy density plumes induced by trawl activity can exceed the natural export of recently deposited material from the shelf and slope (Wollast, 1998). From a climate perspective, the anthropogenic enhancement of sediment transport off shelf to the deeper margin below the permanent thermocline, and hence out of reach from atmospheric influence, has implications for long term carbon sequestration (e.g. Holt et al., 2009).

Whittard canyon, like many other submarine canyons, hosts rich biodiversity (e.g. De Leo 2010; Vetter et al., 2010). Diverse communities of benthic and suspension feeding fauna (Fig. 11) seek refuge and utilise the enhanced food input that is sustained by the canyon morphology (Huvenne et al., 2011; Johnson et al., 2013). It would seem likely that adding such volumes of material will have an influence on the natural biogeochemical status of sinking, food rich particles in the deep-sea (Billet et al., 1983). Some studies have even suggested that anthropogenic modification by trawling can have greater effects than seasonal input of carbon (Sañé et al., 2013).

While Duineveld et al. (2001) and Amaro et al. (2015) also reported episodic events transporting substantial amounts of SPM, the cause of these events was not identified. SPM

concentrations in the two eastern branches (WC3 & 4) varied dramatically (1.2 ±1.3 mg l^{-1}) as well as the OC content and C/N ratios (51.2 ±40.8%; 13.8 ±8 respectively). However, the lipid composition from WC3 & 4 was remarkably similar; with SFAs and alcohols dominating in both samples (SFAs: 36.8 ±1.4%; Alcohols: 46.5 ±6.1%) (Fig. 10). Contrary to that found by Amaro et al. (2015), here many of the individual compounds identified have phytoplankton origins (> 90%) and are a good food source to canyon communities within the eastern branches. Furthermore, C/N values in WC4 were comparable to surface values (7.3 ±1.3), and suggested that at least some of the material is fresh and has been rapidly transported to this depth (1370 m) within the canyon. It is likely these compounds are utilised before reaching the channel of the system (Amaro et al., 2015). The lipid composition from the western branches was notably different and had dramatically lower alcohol content (3.4 ±2.3%) and higher contributions of both MUFAs (53.5 ±8.9%) and PUFAs (10.3 ± 9.3%) (Fig. 10). Huvenne et al. (2011) also reported differences in their lipid compositions between different branches, albeit the samples were also collected at different depths. They attributed differences in the contributions of PUFAs (in the east) and MUFAs (in the west) to variations in the contributions from phytoplankton and zooplankton from/at distinct locations and this may also be the case here. However, our results would suggest that anthropogenic loading should also to be considered when interpreting the biogeochemical signatures within a multi-channel system, particularly given the regional variation in fishing intensity.

Other studies have also found differences between western and eastern branches of the canyon systems in faunal community compositions and abundance (Gunton et al. (2015) and references within) and in sediment characteristics (Duros et al., 2011; 2012; Hunter et al., 2013) and have been related to physical dynamics. Recent modelling and glider observations (Amaro et al., 2016; Aslam et al., 2017) have shown that the heterogeneity of benthic dynamics within Whittard Canyon is large with highly variable energy fluxes (in direction and magnitude) across the various branches. Trawling may input more material into the system and high energy plumes may transport fresh material from shelf regions to greater depths within the canyon, but local dynamics in each branch will also influence the local material transport and spatial heterogeneity in the canyon biogeochemistry. Furthermore, the biogeochemical data presented here only show a snap shot in time. Indeed, although low concentrations of SPM were detected at the site in WC3 (Fig 2. Sample point: S3), the sampling date (14th June 2013) coincided with the detection of trawl induced ENLs in as defined by Wilson et al. (2015a) in this branch. Given this and the high C/N values, these

measurements may be from the remnants of a trawl plume. The initial particle loading and duration since the passage of a trawling plume event will determine the biogeochemical composition of the suspended organic material, which further explains the highly heterogenous C/N values measured here and in ENLs by Wilson et al. (2015a).

Together with the geographic distribution of fishing activity, compositional differences between organic material from western and eastern branches suggest that there may be a zonal trend in anthropogenically introduced sediment supply. However further work is needed, as there was a lack of replicates and the limited number of samples presented here, does not allow for robust statistical analysis of any relationship or difference. There were no statistically significant results for any of the two-sample T-tests (assuming unequal variances) preformed, but there were strong indications that there was a difference between contributions of some lipid groups, (e.g. alcohols $t = -9.3$, $p = 0.07$). Other studies have suggested that lipids are too labile to examine this question (Sañé et al., 2013), but here we have shown that lipids may be used as sensitive biomarkers and may provide greater insight into the alteration of organic material in the canyon by natural and/or trawling processes.

[**Figure 11** here please, at 2 columns wide]

Alterations to the food source may have positive and negative implications depending on the species feeding mechanism/habitat (e.g. Billett et al., 1983; Ramirez-Llodra et al., 2005; Quattrini et al., 2015 and references within). Increased input into the system may favour suspension feeding fauna/fauna living on walls, while benthic organisms may be victim to a food source with less bioavailability and higher degradation at the seabed. Figure 11 presents a set of photo images, in order to visualise the varying conditions experienced by local fauna. Species that are accustomed to low sedimentation rates would be forced to endure any extra deposition introduced by trawl fishing. These are often slow growing and/or niche species susceptible to minor changes in their environment. Although these images cannot infer any impacts from anthropogenic events, they do portray the wide variation of sedimentary settings found. Anthropogenically generated heterogeneity in sediment supply and character will also impact on habitat suitability for resident ecosystems and associated habitat niche modelling (Davies et al., 2014; Robert et al., 2015).

In recent times, the adverse effects of pollution have been realised within the marine realm, for example, from offshore hydrocarbon drill cuttings on delicate cold-water coral habitats (Purser and Thomsen, 2012). Toxic compounds, such as trace metals (e.g. Palanques et al., 2008; Heimbürger et al., 2012; Sousa et al., 2012), along with general marine litter (Tubau et al., 2015), especially micro-plastics, are being increasingly discovered on continental shelves, margins and canyons. If trawling induced plumes can induce enhanced sediment flux across the margin, then equally they have the capacity to accelerate the spread of other anthropogenic processes, such as contamination, from shelf to deep ocean regions. This anthropogenic forcing can be accentuated even further by the funnelling effect of submarine canyons like those found at Whittard Canyon, even when located some distance from the coastal zone.

5. Acknowledgments

This work received support from the Griffiths Project and the Irish Centre for Research in Applied Geoscience (iCRAG) through Science Foundation Ireland (SFI). The authors would like to thank the captain, crews and scientists involved in CE13008 & CE16006. These cruises were funded through the Marine Institute's National Shiptime Programme. The authors gratefully acknowledge Sabena Blackbird (UoL) & Nicola Dempster (LJMU) for their technical assistance with elemental and GC-MS analysis & Emma L. Smith (LJMU) for her lipid biomarker discussions. The authors thank two anonymous reviewers for their comments which significantly improved the later version of the manuscript.

6. References

Amaro, T., de Stigter, H., Lavaleye, M., Duineveld, G., 2015. Organic matter enrichment in the Whittard Channel; its origin and possible effects on benthic megafauna. Deep Sea Research Part I: Oceanographic Research Papers 102, 90–100. https://doi.org/10.1016/j.dsr.2015.04.014

Amaro, T., Huvenne, V.A.I., Allcock, A.L., Aslam, T., Davies, J.S., Danovaro, R., De Stigter, H.C., Duineveld, G.C.A., Gambi, C., Gooday, A.J., Gunton, L.M., Hall, R., Howell, K.L., Ingels, J., Kiriakoulakis, K., Kershaw, C.E., Lavaleye, M.S.S., Robert, K.,

Stewart, H., Van Rooij, D., White, M., Wilson, A.M., 2016. The Whittard Canyon – A case study of submarine canyon processes. Progress in Oceanography 146, 38–57. https://doi.org/10.1016/j.pocean.2016.06.003

Aslam, T., Hall, R., Dye, S., 2017. Internal tides in a dendritic submarine canyon. Progress in Oceanography. [IN PRESS]

Benn, A.R., Weaver, P.P., Billet, D.S., Van Den Hove, S., Murdock, A.P., Doneghan, G.B., Le Bas, T., 2010. Human activities on the deep seafloor in the North East Atlantic: an assessment of spatial extent. PloS one 5, e12730.

Billett, D., Lampitt, R., Rice, A., Mantoura, R., 1983. Seasonal sedimentation of phytoplankton to the deep-sea benthos. Nature 302, 520–522.

Canals, M., Puig, P., de Madron, X.D., Heussner, S., Palanques, A., Fabres, J., 2006. Flushing submarine canyons. Nature 444, 354–357.

Carter, G.S., Gregg, M.C., 2002. Intense, variable mixing near the head of Monterey Submarine Canyon. Journal of Physical Oceanography 32, 3145–3165.

Conte, M., Dickey, T., Weber, J., Johnson, R., Knap, A., 2003. Transient physical forcing of pulsed export of bioreactive material to the deep Sargasso Sea. Deep Sea Research Part I: Oceanographic Research Papers 50, 1157–1187.

Davies, J.S., Howell, K.L., Stewart, H.A., Guinan, J., Golding, N., 2014. Defining biological assemblages (biotopes) of conservation interest in the submarine canyons of the South West Approaches (offshore United Kingdom) for use in marine habitat mapping. Deep Sea Research Part II: Topical Studies in Oceanography 104, 208–229. https://doi.org/10.1016/j.dsr2.2014.02.001

Davies, A.J., Roberts, J.M., Hall-Spencer, J., 2007. Preserving deep-sea natural heritage: emerging issues in offshore conservation and management. Biological Conservation 138, 299–312.

De Leo, F.C., Smith, C.R., Rowden, A.A., Bowden, D.A., Clark, M.R., 2010. Submarine canyons: hotspots of benthic biomass and productivity in the deep sea. Proceedings of the Royal Society of London B: Biological Sciences rspb20100462.

Dillon, T., 1982. Vertical overturns: A comparison of Thorpe and Ozmidov length scales. Journal of Geophysical Research: Oceans 87, 9601–9613.

Doney, S.C., 2010. The growing human footprint on coastal and open-ocean biogeochemistry. science 328, 1512–1516.

Du Preez, C., 2015. A new arc-chord ratio (ACR) rugosity index for quantifying three-dimensional landscape structural complexity. Landscape ecology 30, 181.

Duineveld, G., Lavaleye, M., Berghuis, E., De Wilde, P., 2001. Activity and composition of the benthic fauna in the Whittard Canyon and the adjacent continental slope (NE Atlantic). Oceanologica Acta 24, 69–83.

Duineveld, G.C., Jeffreys, R.M., Lavaleye, M.S., Davies, A.J., Bergman, M.J., Watmough, T., Witbaard, R., 2012. Spatial and tidal variation in food supply to shallow cold-water coral reefs of the Mingulay Reef complex (Outer Hebrides, Scotland). Marine Ecology Progress Series 444, 97–115.

Dunn, D., Halpin, P., 2009. Rugosity-based regional modeling of hard-bottom habitat. Marine Ecology Progress Series 377, 1–11. https://doi.org/10.3354/meps07839

Duros, P., Fontanier, C., de Stigter, H.C., Cesbron, F., Metzger, E., Jorissen, F.J., 2012. Live and dead benthic foraminiferal faunas from Whittard Canyon (NE Atlantic): Focus on

taphonomic processes and paleo-environmental applications. Marine Micropaleontology 94–95, 25–44. https://doi.org/10.1016/j.marmicro.2012.05.004

Duros, P., Fontanier, C., Metzger, E., Pusceddu, A., Cesbron, F., de Stigter, H.C., Bianchelli, S., Danovaro, R., Jorissen, F.J., 2011. Live (stained) benthic foraminifera in the Whittard Canyon, Celtic margin (NE Atlantic). Deep Sea Research Part I: Oceanographic Research Papers 58, 128–146. https://doi.org/10.1016/j.dsr.2010.11.008

Eastwood, P.D., Mills, C.M., Aldridge, J.N., Houghton, C.A., Rogers, S.I., 2007. Human activities in UK offshore waters: an assessment of direct, physical pressure on the seabed. ICES J Mar Sci 64, 453–463. https://doi.org/10.1093/icesjms/fsm001

(EU) Council Regulation 2016/2336 of 14th December 2016 establishing specific conditions for fishing for deep-sea stocks in the north-east Atlantic and provisions for fishing in international waters of the north-east Atlantic and repealing Council Regulation (EC) No 2347/2002 (OJ L 354, 23.12.2016, p. 2)

Galbraith, P.S., Kelley, D.E., 1996. Identifying overturns in CTD profiles. Journal of Atmospheric and Oceanic Technology 13, 688–702.

Gerritsen, H., Lordan, C., 2011. Integrating vessel monitoring systems (VMS) data with daily catch data from logbooks to explore the spatial distribution of catch and effort at high resolution. ICES Journal of Marine Science 68, 245–252. https://doi.org/10.1093/icesjms/fsq137

Gerritsen, H.D., Minto, C., Lordan, C., 2013. How much of the seabed is impacted by mobile fishing gear? Absolute estimates from Vessel Monitoring System (VMS) point data. ICES Journal of Marine Science 70, 523–531.

Grassle, J.F., Maciolek, N.J., 1992. Deep-sea species richness: regional and local diversity estimates from quantitative bottom samples. The American Naturalist 139, 313–341.

Gregg, M.C., Carter, G.S., Kunze, E., 2005. CORRIGENDUM. Journal of Physical Oceanography 35, 1712–1715. https://doi.org/10.1175/JPO2789.1

Gunton, L.M., Gooday, A.J., Glover, A.G., Bett, B.J., 2015. Macrofaunal abundance and community composition at lower bathyal depths in different branches of the Whittard Canyon and on the adjacent slope (3500m; NE Atlantic). Deep Sea Research Part I: Oceanographic Research Papers 97, 29–39. https://doi.org/10.1016/j.dsr.2014.11.010

Hall, R.A., Aslam, T., Huvenne, V.A.I., 2017. Partly standing internal tides in a dendritic submarine canyon observed by an ocean glider. Deep Sea Research Part I: Oceanographic Research Papers. https://doi.org/10.1016/j.dsr.2017.05.015

Halpern, B.S., Walbridge, S., Selkoe, K.A., Kappel, C.V., Micheli, F., D'Agrosa, C., Bruno, J.F., Casey, K.S., Ebert, C., Fox, H.E., Fujita, R., Heinemann, D., Lenihan, H.S., Madin, E.M.P., Perry, M.T., Selig, E.R., Spalding, M., Steneck, R., Watson, R., 2008. A Global Map of Human Impact on Marine Ecosystems. Science 319, 948–952. https://doi.org/10.1126/science.1149345

Harwood, J.L., Russell, N.L., 1984. Lipids in Plants and Microorganisms. George Allen and Unwin, London.

Heimbürger, L.-E., Cossa, D., Thibodeau, B., Khripounoff, A., Mas, V., Chiffoleau, J.-F., Schmidt, S., Migon, C., 2012. Natural and anthropogenic trace metals in sediments of the Ligurian Sea (Northwestern Mediterranean). Chemical Geology 291, 141–151. https://doi.org/10.1016/j.chemgeo.2011.10.011

Holt, J., Wakelin, S., Huthnance, J., 2009. Down-welling circulation of the northwest European continental shelf: A driving mechanism for the continental shelf carbon pump. Geophysical Research Letters 36.

Hunter, W.R., Jamieson, A., Huvenne, V.A.I., Witte, U., 2013. Sediment community responses to marine vs. terrigenous organic matter in a submarine canyon. Biogeosciences 10, 67–80. https://doi.org/10.5194/bg-10-67-2013

Huvenne, V.A., Tyler, P.A., Masson, D.G., Fisher, E.H., Hauton, C., Hühnerbach, V., Le Bas, T.P., Wolff, G.A., 2011. A picture on the wall: innovative mapping reveals cold-water coral refuge in submarine canyon. PloS one 6, e28755.

Johnson, M.P., White, M., Wilson, A., Würzberg, L., Schwabe, E., Folch, H., Allcock, A.L., 2013. A vertical wall dominated by Acesta excavata and Neopycnodonte zibrowii, part of an undersampled group of deep-sea habitats. PloS one 8, e79917.

Jones, J., 1992. Environmental impact of trawling on the seabed: a review. New Zealand Journal of Marine and Freshwater Research 26, 59–67.

Kaiser, M.J., Collie, J.S., Hall, S.J., Jennings, S., Poiner, I.R., 2002. Modification of marine habitats by trawling activities: prognosis and solutions. Fish and Fisheries 3, 114–136. https://doi.org/10.1046/j.1467-2979.2002.00079.x

Khripounoff, A., Vangriesheim, A., Crassous, P., Etoubleau, J., 2009. High frequency of sediment gravity flow events in the Var submarine canyon (Mediterranean Sea). Marine Geology 263, 1–6. https://doi.org/10.1016/j.margeo.2009.03.014

Kiriakoulakis, K., Blackbird, S., Ingels, J., Vanreusel, A., Wolff, G.A., 2011. Organic geochemistry of submarine canyons: The Portuguese Margin. Deep Sea Research Part II: Topical Studies in Oceanography 58, 2477–2488. https://doi.org/10.1016/j.dsr2.2011.04.010

Kiriakoulakis, K., Freiwald, A., Fisher, E., Wolff, G., 2007. Organic matter quality and supply to deep-water coral/mound systems of the NW European Continental Margin. International Journal of Earth Sciences 96, 159–170.

Kiriakoulakis, K., Marshall, J., Wolff, G., 2000. Biomarkers in a Lower Jurassic concretion from Dorset (UK). Journal of the Geological Society 157, 207–220.

Kiriakoulakis, K., Vilas, J.C., Blackbird, S.J., Arístegui, J., Wolff, G.A., 2009. Seamounts and organic matter—Is there an effect? The case of Sedlo and Seine seamounts, Part 2. Composition of suspended particulate organic matter. Deep Sea Research Part II: Topical Studies in Oceanography 56, 2631–2645. https://doi.org/10.1016/j.dsr2.2008.12.024

Koenig, S., Fernández, P., Company, J.B., Huertas, D., Solé, M., 2013. Are deep-sea organisms dwelling within a submarine canyon more at risk from anthropogenic contamination than those from the adjacent open slope? A case study of Blanes canyon (NW Mediterranean). Progress in Oceanography 118, 249–259. https://doi.org/10.1016/j.pocean.2013.07.016

Lee, I.-H., Lien, R.-C., Liu, J.T., Chuang, W., 2009. Turbulent mixing and internal tides in Gaoping (Kaoping) submarine canyon, Taiwan. Journal of Marine Systems 76, 383–396.

Levin, L.A., Dayton, P.K., 2009. Ecological theory and continental margins: where shallow meets deep. Trends in ecology & evolution 24, 606–617.

Levin, L.A., Sibuet, M., 2012. Understanding continental margin biodiversity: a new imperative. Annual Review of Marine Science 4, 79–112.

Levin, L.A., Sibuet, M., Gooday, A.J., Smith, C.R., Vanreusel, A., 2010. The roles of habitat heterogeneity in generating and maintaining biodiversity on continental margins: an introduction. Marine Ecology 31, 1–5.

MacDonald, D.G., Carlson, J., Goodman, L., 2013. On the heterogeneity of stratified-shear turbulence: Observations from a near-field river plume. Journal of Geophysical Research: Oceans 118, 6223–6237.

Martín, J., Puig, P., Masqué, P., Palanques, A., Sánchez-Gómez, A., 2014a. Impact of bottom trawling on deep-sea sediment properties along the flanks of a submarine canyon. PloS one 9, e104536.

Martín, J., Puig, P., Palanques, A., Giamportone, A., 2014b. Commercial bottom trawling as a driver of sediment dynamics and deep seascape evolution in the Anthropocene. Anthropocene 7, 1–15. https://doi.org/10.1016/j.ancene.2015.01.002

Martín, J., Puig, P., Palanques, A., Masqué, P., García-Orellana, J., 2008. Effect of commercial trawling on the deep sedimentation in a Mediterranean submarine canyon. Marine Geology 252, 150–155.

Martín, J., Puig, P., Palanques, A., Ribó, M., 2014c. Trawling-induced daily sediment resuspension in the flank of a Mediterranean submarine canyon. Deep Sea Research Part II: Topical Studies in Oceanography, Submarine Canyons: Complex Deep-Sea Environments Unravelled by Multidisciplinary Research 104, 174–183. https://doi.org/10.1016/j.dsr2.2013.05.036

Mater, B.D., Schaad, S.M., Venayagamoorthy, S.K., 2013. Relevance of the Thorpe length scale in stably stratified turbulence. Physics of Fluids 25, 076604.

Mater, B.D., Venayagamoorthy, S.K., St. Laurent, L., Moum, J.N., 2015. Biases in Thorpe-scale estimates of turbulence dissipation. Part I: Assessments from large-scale overturns in oceanographic data. Journal of Physical Oceanography 45, 2497–2521.

Morato, T., Watson, R., Pitcher, T.J., Pauly, D., 2006. Fishing down the deep. Fish and fisheries 7, 24–34.

Nédélec, C., Prado, J., 1990. Definition and classification of fishing gear categories. Définition et classification des categories d'engins de péche. Definición y clasificación de las diversas categorías de artes de pesca. FAO Fisheries Technical Paper.

Oberle, F.K.J., Storlazzi, C.D., Hanebuth, T.J.J., 2016a. What a drag: Quantifying the global impact of chronic bottom trawling on continental shelf sediment. Journal of Marine Systems 159, 109–119. https://doi.org/10.1016/j.jmarsys.2015.12.007

Oberle, F.K.J., Swarzenski, P.W., Reddy, C.M., Nelson, R.K., Baasch, B., Hanebuth, T.J.J., 2016b. Deciphering the lithological consequences of bottom trawling to sedimentary habitats on the shelf. Journal of Marine Systems 159, 120–131. https://doi.org/10.1016/j.jmarsys.2015.12.008

O'Neill, F.G., Summerbell, K., 2011. The mobilisation of sediment by demersal otter trawls. Marine Pollution Bulletin 62, 1088–1097. https://doi.org/10.1016/j.marpolbul.2011.01.038

Palanques, A., 1994. Distribution and heavy metal pollution of the suspended particulate matter on the Barcelona continental shelf (North-Western Mediterranean). Environmental Pollution 85, 205–215.

Palanques, A., Martín, J., Puig, P., Guillén, J., Company, J.B., Sardà, F., 2006. Evidence of sediment gravity flows induced by trawling in the Palamós (Fonera) submarine canyon

(northwestern Mediterranean). Deep Sea Research Part I: Oceanographic Research Papers 53, 201–214. https://doi.org/10.1016/j.dsr.2005.10.003

Palanques, A., Masqué, P., Puig, P., Sanchez-Cabeza, J.A., Frignani, M., Alvisi, F., 2008. Anthropogenic trace metals in the sedimentary record of the Llobregat continental shelf and adjacent Foix Submarine Canyon (northwestern Mediterranean). Marine Geology 248, 213–227. https://doi.org/10.1016/j.margeo.2007.11.001

Palanques, A., Puig, P., Guillén, J., Demestre, M., Martín, J., 2014. Effects of bottom trawling on the Ebro continental shelf sedimentary system (NW Mediterranean). Continental Shelf Research 72, 83–98.

Payo-Payo, M., Jacinto, R., Lastras, G., Rabineau, M., Puig, P., Martín, J., Canals, M., Sultan, N., 2017. Numerical modeling of bottom trawling-induced sediment transport and accumulation in La Fonera submarine canyon, northwestern Mediterranean Sea. Marine Geology 386, 107–125.

Pham, C.K., Ramirez-Llodra, E., Alt, C.H., Amaro, T., Bergmann, M., Canals, M., Davies, J., Duineveld, G., Galgani, F., Howell, K.L., 2014. Marine litter distribution and density in European seas, from the shelves to deep basins. PLoS One 9, e95839.

Pilskaln, C.H., Churchill, J.H., Mayer, L.M., 1998. Resuspension of sediment by bottom trawling in the Gulf of Maine and potential geochemical consequences. Conservation Biology 12, 1223–1229.

Puig, P., Canals, M., Company, J.B., Martin, J., Amblas, D., Lastras, G., Palanques, A., Calafat, A.M., 2012. Ploughing the deep sea floor. Nature 489, 286–289. https://doi.org/10.1038/nature11410

Puig, P., Palanques, A., Martín, J., 2014. Contemporary Sediment-Transport Processes in Submarine Canyons. Annual Review of Marine Science 6, 53–77. https://doi.org/10.1146/annurev-marine-010213-135037

Purser, A., Thomsen, L., 2012. Monitoring strategies for drill cutting discharge in the vicinity of cold-water coral ecosystems. Marine Pollution Bulletin 64, 2309–2316. https://doi.org/10.1016/j.marpolbul.2012.08.003

Pusceddu, A., Bianchelli, S., Martín, J., Puig, P., Palanques, A., Masqué, P., Danovaro, R., 2014. Chronic and intensive bottom trawling impairs deep-sea biodiversity and ecosystem functioning. Proceedings of the National Academy of Sciences 111, 8861–8866.

Pusceddu, A., Fiordelmondo, C., Danovaro, R., 2005a. Sediment resuspension effects on the benthic microbial loop in experimental microcosms. Microbial ecology 50, 602–613.

Pusceddu, A., Fiordelmondo, C., Polymenakou, P., Polychronaki, T., Tselepides, A., Danovaro, R., 2005b. Effects of bottom trawling on the quantity and biochemical composition of organic matter in coastal marine sediments (Thermaikos Gulf, northwestern Aegean Sea). Continental Shelf Research 25, 2491–2505.

Quattrini, A.M., Nizinski, M.S., Chaytor, J.D., Demopoulos, A.W.J., Roark, E.B., France, S.C., Moore, J.A., Heyl, T., Auster, P.J., Kinlan, B., Ruppel, C., Elliott, K.P., Kennedy, B.R.C., Lobecker, E., Skarke, A., Shank, T.M., 2015. Exploration of the Canyon-Incised Continental Margin of the Northeastern United States Reveals Dynamic Habitats and Diverse Communities. PLOS ONE 10, e0139904. https://doi.org/10.1371/journal.pone.0139904

Ramirez-Llodra, E., Tyler, P.A., Baker, M.C., Bergstad, O.A., Clark, M.R., Escobar, E., Levin, L.A., Menot, L., Rowden, A.A., Smith, C.R., 2011. Man and the last great wilderness: human impact on the deep sea. PLoS One 6, e22588.

Reid, G.., Hamilton, D., 1990. A reconnaissance survey of the Whittard Sea Fan, Southwestern Approaches, British Isles. Marine Geology 92, 69–86. https://doi.org/10.1016/0025-3227(90)90027-H

Robert, K., Jones, D.O.B., Tyler, P.A., Van Rooij, D., Huvenne, V.A.I., 2015. Finding the hotspots within a biodiversity hotspot: fine-scale biological predictions within a submarine canyon using high-resolution acoustic mapping techniques. Mar Ecol 36, 1256–1276. https://doi.org/10.1111/maec.12228

Sanchez-Vidal, A., Canals, M., Calafat, A.M., Lastras, G., Pedrosa-Pàmies, R., Menéndez, M., Medina, R., Hereu, B., Romero, J., Alcoverro, T., 2012. Impacts on the deep-sea ecosystem by a severe coastal storm. PLoS One 7, e30395.

Sañé, E., Martín, J., Puig, P., Palanques, A., 2013. Organic biomarkers in deep-sea regions affected by bottom trawling: pigments, fatty acids, amino acids and carbohydrates in surface sediments from the La Fonera (Palamós) Canyon, NW Mediterranean Sea. Biogeosciences 10, 8093.

Sharples, J., Scott, B.E., Inall, M.E., 2013. From physics to fishing over a shelf sea bank. Progress in Oceanography 117, 1–8. https://doi.org/10.1016/j.pocean.2013.06.015

Sousa, A.C.A., Oliveira, I.B., Laranjeiro, F., Takahashi, S., Tanabe, S., Cunha, M.R., Barroso, C.M., 2012. Organotin levels in Nazaré canyon (west Iberian Margin, NE Atlantic) and adjacent coastal area. Marine Pollution Bulletin 64, 422–426. https://doi.org/10.1016/j.marpolbul.2011.11.013

Thorpe, S., 1977. Turbulence and mixing in a Scottish loch. Philosophical Transactions of the Royal Society of London A: Mathematical, Physical and Engineering Sciences 286, 125–181.

Tubau, X., Canals, M., Lastras, G., Rayo, X., Rivera, J., Amblas, D., 2015. Marine litter on the floor of deep submarine canyons of the Northwestern Mediterranean Sea: The role of hydrodynamic processes. Progress in Oceanography 134, 379–403. https://doi.org/10.1016/j.pocean.2015.03.013

Van Weering, T.C., Hall, I., De Stigter, H., McCave, I., Thomsen, L., 1998. Recent sediments, sediment accumulation and carbon burial at Goban Spur, NW European Continental Margin (47–50 N). Progress in Oceanography 42, 5–35.

Vetter, E.W., Smith, C.R., De Leo, F.C., 2010. Hawaiian hotspots: enhanced megafaunal abundance and diversity in submarine canyons on the oceanic islands of Hawaii. Marine Ecology 31, 183–199.

Volkman, J., Johns, R., 1977. The geochemical significance of positional isomers of unsaturated acids from an intertidal zone sediment. Nature 267, 693–694.

Volkman, J.K., Barrett, S.M., Blackburn, S.I., Mansour, M.P., Sikes, E.L., Gelin, F., 1998. Microalgal biomarkers: a review of recent research developments. Organic Geochemistry 29, 1163–1179.

Watling, L., Norse, E.A., 1998. Disturbance of the Seabed by Mobile Fishing Gear: A Comparison to Forest Clearcutting. Conservation Biology 12, 1180–1197. https://doi.org/10.1046/j.1523-1739.1998.0120061180.x

Wilson, A.M., Kiriakoulakis, K., Raine, R., Gerritsen, H.D., Blackbird, S., Allcock, A.L., White, M., 2015a. Anthropogenic influence on sediment transport in the Whittard

Canyon, NE Atlantic. Marine Pollution Bulletin 101, 320–329. https://doi.org/10.1016/j.marpolbul.2015.10.067

Wilson, A.M., Raine, R., Mohn, C., White, M., 2015b. Nepheloid layer distribution in the Whittard Canyon, NE Atlantic Margin. Marine Geology 367, 130–142. https://doi.org/10.1016/j.margeo.2015.06.002

Wilson, M.F.J., O'Connell, B., Brown, C., Guinan, J.C., Grehan, A.J., 2007. Multiscale Terrain Analysis of Multibeam Bathymetry Data for Habitat Mapping on the Continental Slope. Marine Geodesy 30, 3–35. https://doi.org/10.1080/01490410701295962

Wollast, R., 1998. Evaluation and comparison of the global carbon cycle in the coastal zone and in the open ocean. The sea 10, 213–252.

Wollast, R., Chou, L., 2001. The carbon cycle at the ocean margin in the northern Gulf of Biscay. Deep Sea Research Part II: Topical Studies in Oceanography 48, 3265–3293.

Wood, S., 2017. mgcv: Mixed GAM Computation Vehicle with GCV/AIC/REML smoothness estimation.

Wood, S., 2006. Generalized Additive Models: An Introduction with R. CRC Press.

Wood, S.N., Augustin, N.H., 2002. GAMs with integrated model selection using penalized regression splines and applications to environmental modelling. Ecological modelling 157, 157–177.

Xu, J., Noble, M., Rosenfeld, L.K., 2004. In-situ measurements of velocity structure within turbidity currents. Geophysical Research Letters 31.

Yamamuro, M., Kayanne, H., 1995. Rapid direct determination of organic carbon and nitrogen in carbonate-bearing sediments with a Yanaco MT-5 CHN analyzer. Limnology and Oceanography 40, 1001–1005.

Figure captions

Fig. 1. General overview of the Celtic Margin off the northwest European Continental Shelf. The red box is Fig. 2: Whittard Canyon. Image reproduced from the GEBCO world map 2014, www.gebco.net

Fig. 2. Area map of Whittard Canyon: (a) showing contoured bathymetry (in blue), SPM sample location labels: Ss = surface SPM; S1–4 = SPM samples from WC1–4 and turbulent energy analysis locations: K8 (Fig. 8) & K9 (Fig. 9). (b) bathymetry overlaid with bottom trawling fishing hours from light in yellow to heavy in brown, with a minimum of 10 hrs shown.

Fig. 3. (a) Map image of slope angle at Whittard Canyon, with areas in red being greater than 20°. (b): Map image of ACR rugosity index; contours of VMS fishing effort are superimposed at 10 h (brown) and 100 h (green).

Fig. 4. ACR Rugosity against slope angle for all VMS grid cells split between high (purple) and low (orange) fishing by their median.

Fig. 5. Canyon branch WC3: Standard deviation of rugosity among grid cells for the heavier fished (purple) and lighter fished (orange) data points. Split between 'heavy' and 'light' fishing on the basis of the median VMS fishing value. [Colour for online publishing]

Fig. 5. Canyon branch WC3: Standard deviation of rugosity among grid cells for the heavier fished (solid) and lighter fished (dashed) data points. Split between 'heavy' and 'light' fishing on the basis of the median VMS fishing value. [Black and white for print]

Fig. 6. (a) Geographical representation of data points with contours of predicted residual variation rugosity as output by GAMs package mgcv (Wood, 2017). (b) Partial residual plot showing the combined influence of fishing effort and slope on rugosity. Contours of rugosity indicate the GAM fit to data for the whole Whittard Canyon region, controlling for the other predictors in the best model. Points indicate the distribution of observations for each predictor.

Fig. 7. (a) Along channel section of SPM concentration (mg l^{-1}) in WC4 in the immediate aftermath of a trawling plume, showing the 0.3 and 1 mg l^{-1} contours only. For comparison the hatched area indicates the regions where SPM concentrations > 0.3 mg l^{-1} were measured in other canyon branches when no trawling plumes were evident during the survey. The station locations are shown by the 'x'. In (b), selected vertical profiles of SPM for the above section are indicated in the thick line with thin line showing examples from the same depth in unaffected branches.

Fig. 8. Vertical profiles of (a) σ_t, (b) SPM (mg l^{-1}), (c) Individual Thorpe displacements (m), (d) Thorpe Length Scale for overturns (m) and (e) $\log_{10}$ of the turbulent energy dissipation (ε, W kg^{-1}), for the WC4 location at ~ 1380 water depth in 2016 (see Fig. 2a; K8). (f-j) are the corresponding profiles at the same location during a plume event 31 hours later. Note in (g), the SPM scale is cut off at 5 mg l^{-1}, for clarity – the maximum value in the near bottom turbid layer was 8 mg l^{-1}.

Fig. 9. Vertical profiles of (a) σ_t, (b) SPM (mg l^{-1}), (c) Individual Thorpe displacements (m), (d) Thorpe Length Scale for overturns (m) and (e) $\log_{10}$ of the turbulent energy dissipation (ε, W kg^{-1}), for the WC3 location at ~ 1385 water depth, 2013 (see Fig. 2a; K9).

Fig. 10. Map image showing concentrations of total lipids normalised to volume of water (ng l^{-1}) detected in suspended particulate organic matter collected in four branches (WC1 – 4) and at the surface of Whittard Canyon in June 2013. Pie charts show the contribution of saturated fatty acids, monounsaturated fatty acids (MUFAs), polyunsaturated fatty acids (PUFAs) and fatty alcohols in each sample (locations: S1 – 4 and surface sample Ss; see Fig. 2a).

Fig. 11. Photo images from Whittard Canyon 2013 – 2016, displaying contrasting sediment concentrations both in the water column and resettling on benthic fauna. (a1): Cloudy water surrounds a Brisingid starfish; WC3. (a2): Very clear water and a Flytrap anemone; WC1. (b1): Sediment laden *Acesta excavata*; WC3. (b2): Clean *A. excavata*; WC3. (c1): The soft coral Anthomastus topped with a vail of sediment; WC3. (c2): An Anthomastus perched on a canyon wall with polyps fully extended. Note that the Anthomastus (c1) with retracted polyps may have become sediment covered during earlier ROV manoeuvres adjacent to site (visibility was not sufficient to determine this from the video), but the quantity of loose sediment available for such coverage may have been introduced by trawling.

Table captions

Table 1. Generalised Additive Model (GAM) fits to predict rugosity values in the full dataset, excluding cells with zero fishing (n = 6241 grid cells). Model predictors: R = Rugosity, Ln = longitude, Lt = Latitude, V = VMS fishing hours, S = slope angle. Variables in brackets have been modelled as interacting predictors. Generalised Cross Validation (GCV) scores indicate the relative performance of models, with lower values indicating better fits. Adjusted R^2 values are a less robust indicator of model fit, but are included as their interpretation is more intuitive as an indicator of the performance of models at fitting the data.

Table 2. Fishing intensity (hrs/km^2) for each canyon branch, showing results for whole branches and also broken down into specific areas within branch.

Table 3. Biogeochemical data for four samples (Locations S1 – 4; see Fig. 2a) & the surface sample (Ss) used in this study with mean ± standard deviation for Western and Eastern samples. SPM: suspended particulate matter; C:N: molar carbon to nitrogen ratio; MUFA: monounsaturated fatty acids; PUFA: polyunsaturated fatty acids. Individual compounds, lipid group and primary biomarkers used for indices are shown in the Appendix. * indicates torn filters.

Supplementary Table 1/Appendix: List of compounds most commonly identified in this study with groups and their corresponding IUPAC names. Individual compounds used for the phytoplankton and bacterial indices are indicated.

Figures and Tables:

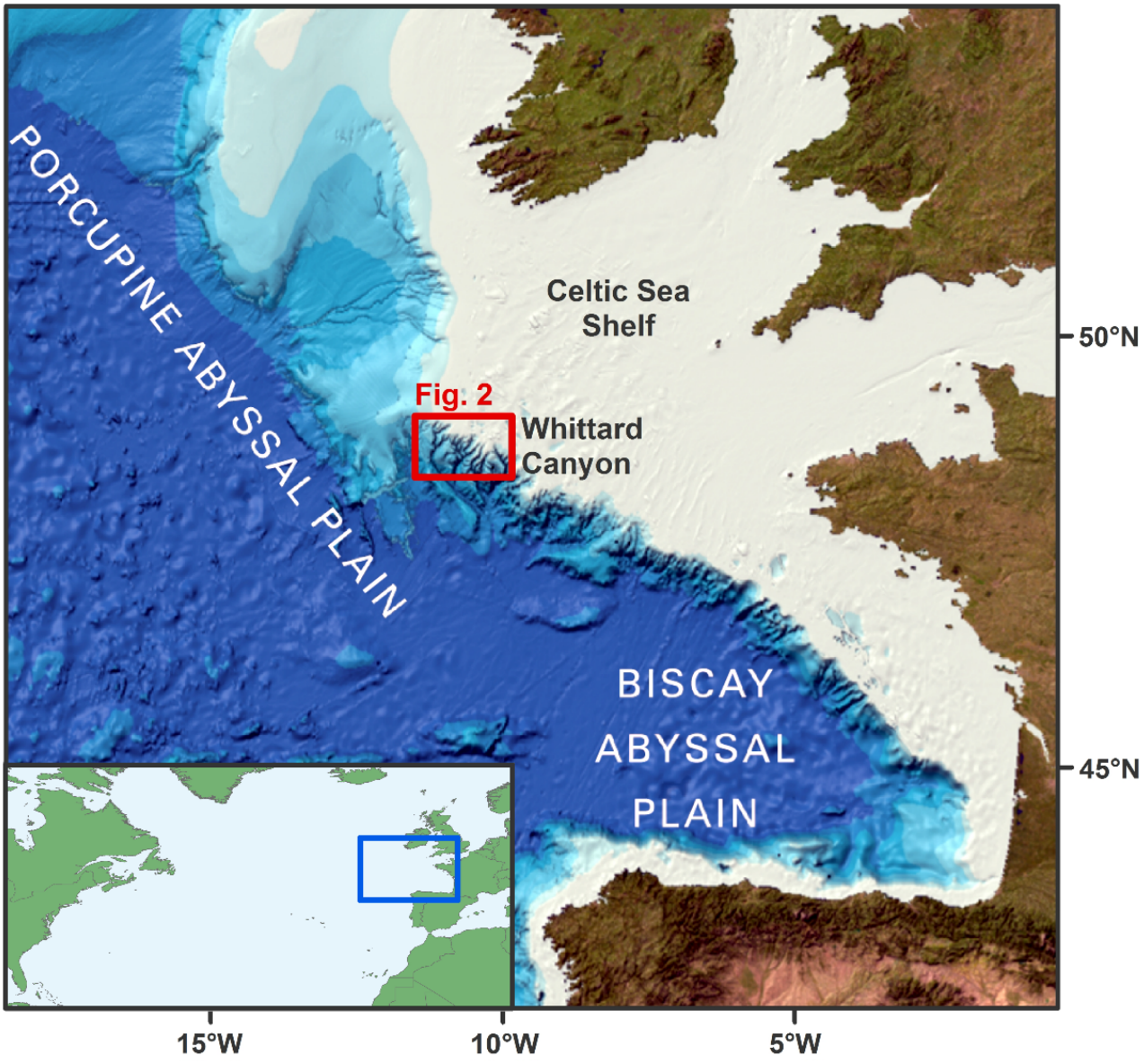

Fig. 1. General overview of the Celtic Margin off the northwest European Continental Shelf. The red box is Fig. 2: Whittard Canyon. Image reproduced from the GEBCO world map 2014, www.gebco.net [1.5 columns wide]

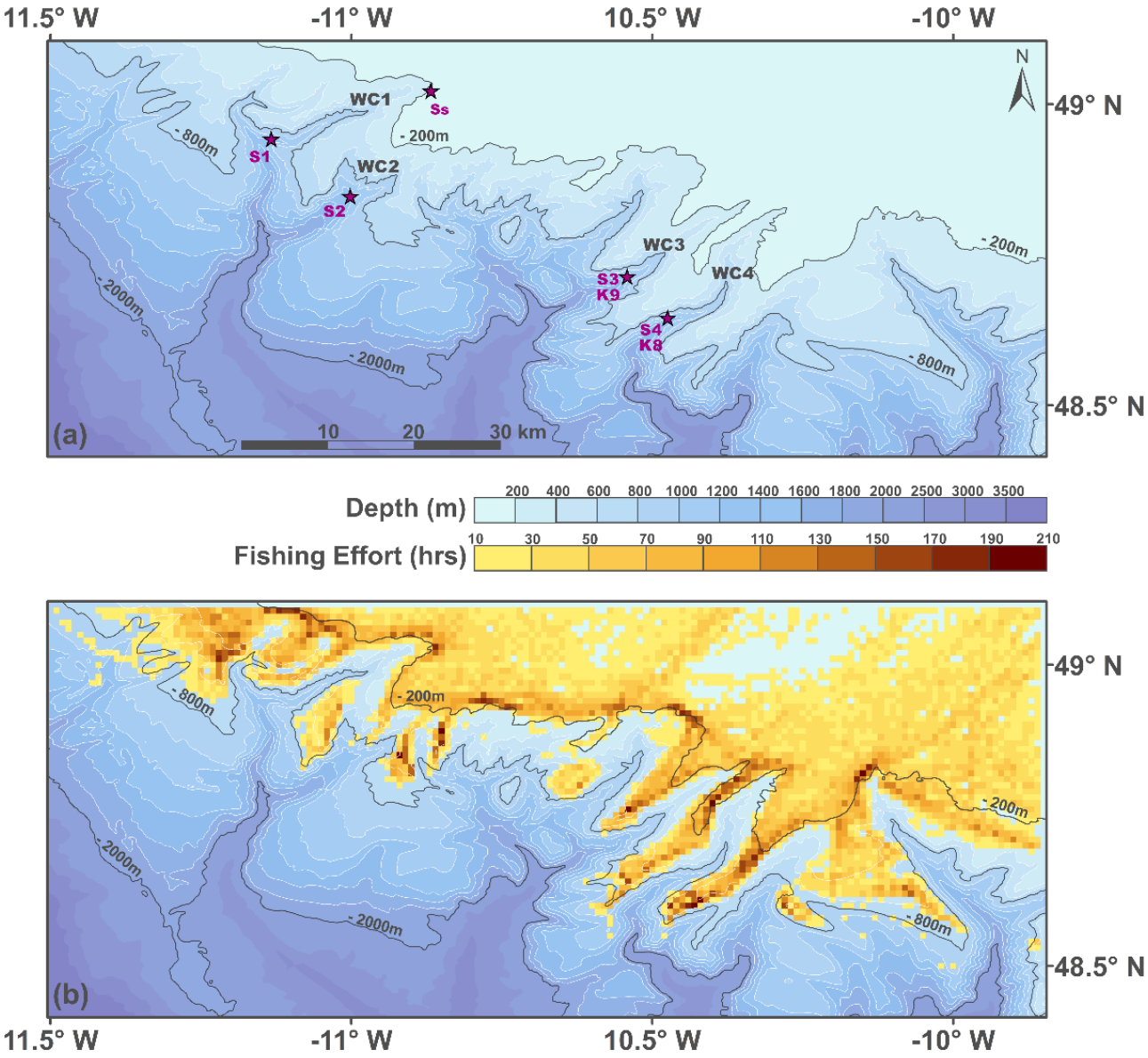

Fig. 2. Area map of Whittard Canyon: (a) showing contoured bathymetry (in blue), SPM sample location labels: Ss = surface SPM; S1–4 = SPM samples from WC1–4 and turbulent energy analysis locations: K8 (Fig. 8) & K9 (Fig. 9). (b) bathymetry overlaid with bottom trawling fishing hours from light in yellow to heavy in brown, with a minimum of 10 hrs shown. [1.5 columns wide]

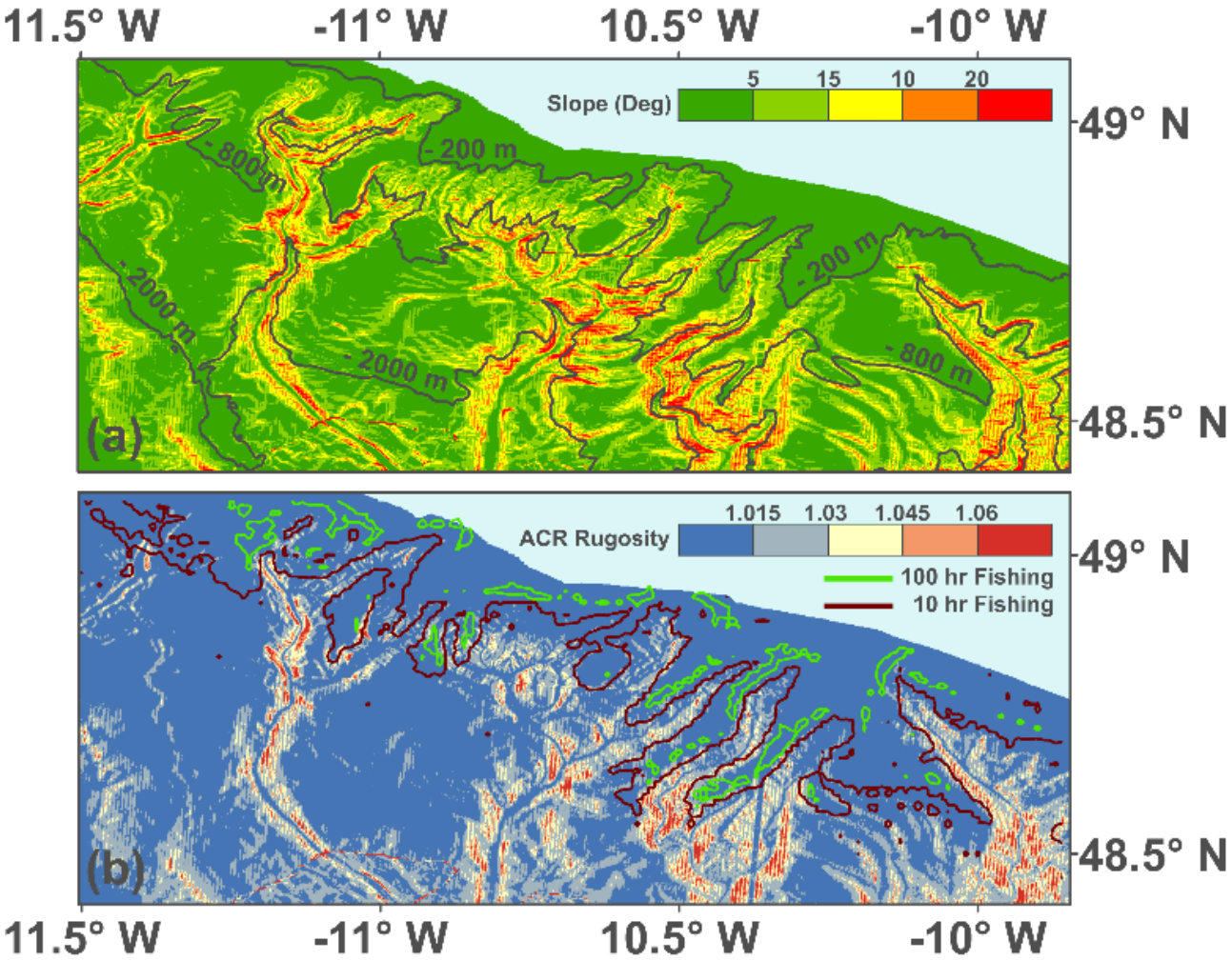

Fig. 3. (a) Map image of slope angle at Whittard Canyon, with areas in red greater than 20°. (b): Map image of ACR rugosity index; contours of VMS fishing effort are superimposed at 10 h (brown) and 100 h (green). [One column wide]

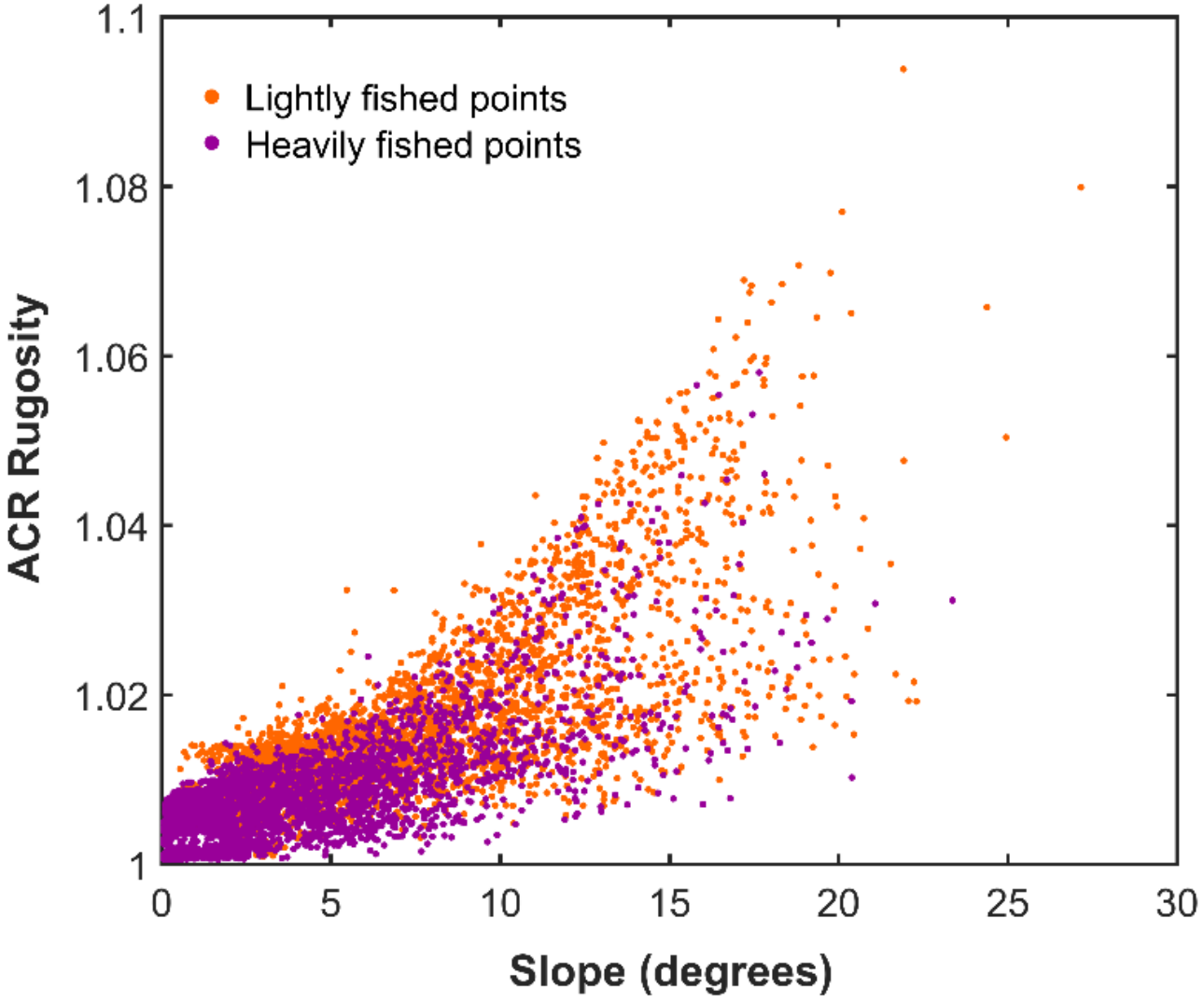

Fig. 4. ACR Rugosity against slope angle for all VMS grid cells split between high (purple) and low (orange) fishing by their median. [One column wide]

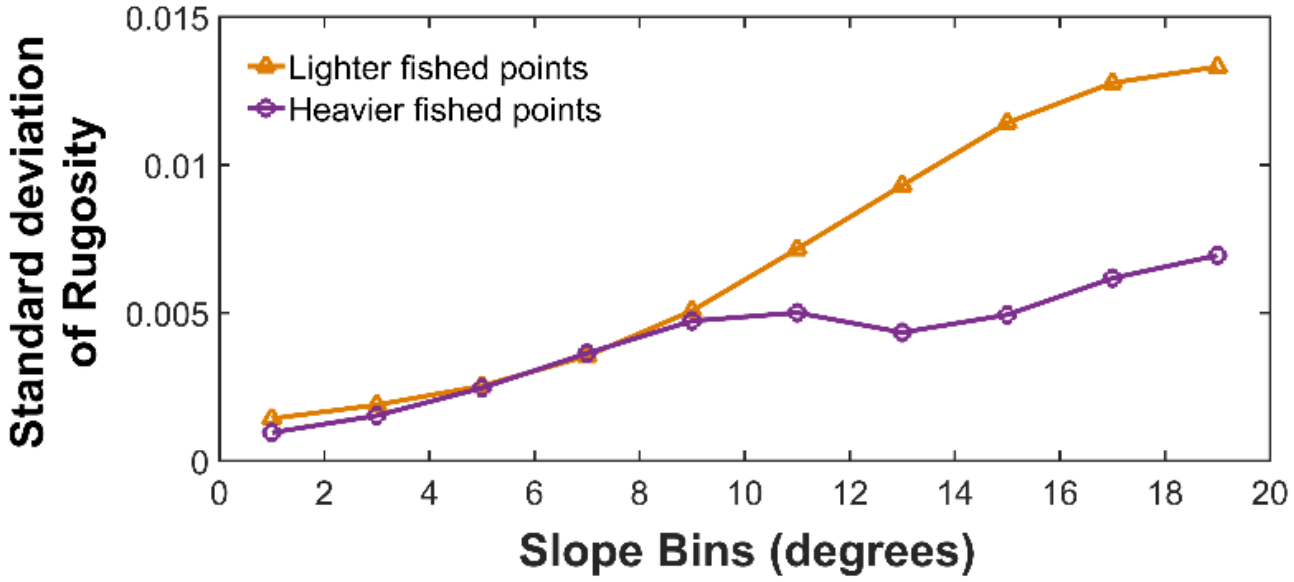

Fig. 5. Canyon branch WC3: Standard deviation of rugosity among grid cells for the heavier fished (purple) and lighter fished (orange) data points. Split between 'heavy' and 'light' fishing on the basis of the median VMS fishing value. [One column wide, for online publishing]

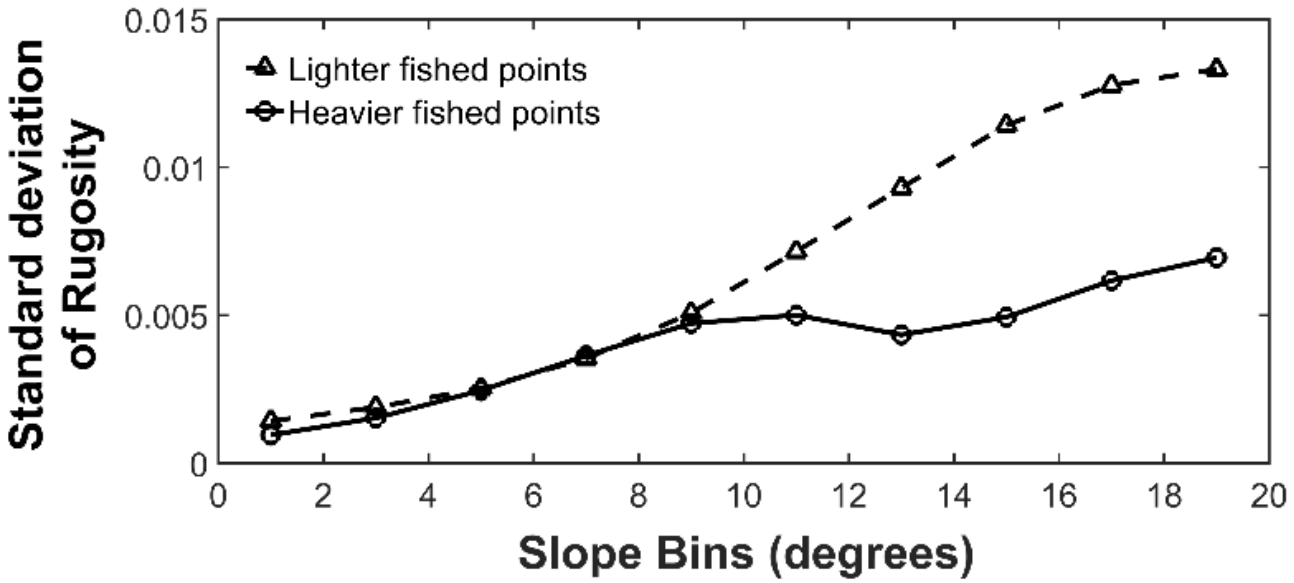

Fig. 5. Canyon branch WC3: Standard deviation of rugosity among grid cells for the heavier fished (solid) and lighter fished (dashed) data points. Split between 'heavy' and 'light' fishing on the basis of the median VMS fishing value. [One column wide, for printing]

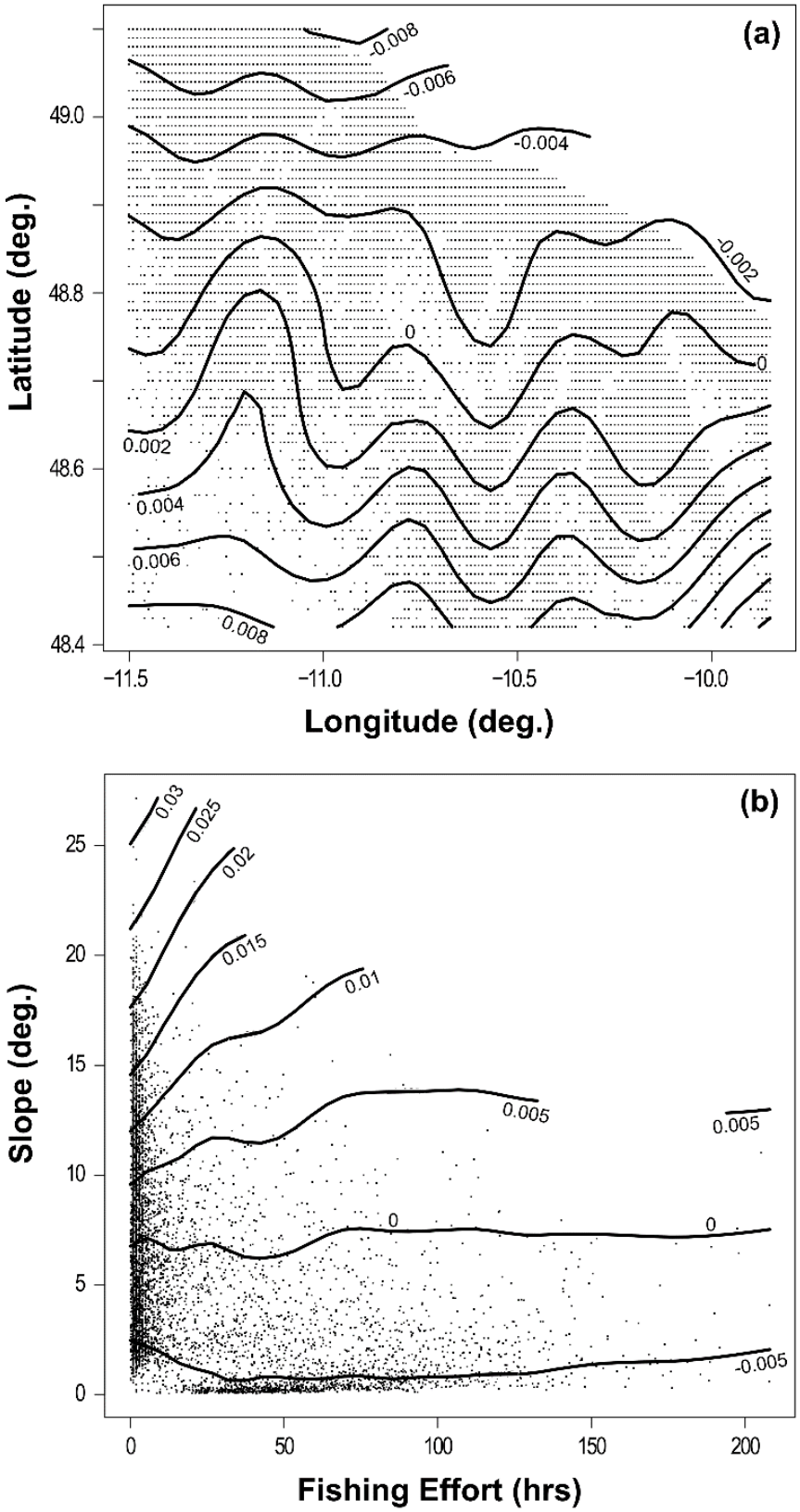

Fig. 6. (a) Geographical representation of data points with contours of predicted residual variation rugosity as output by GAMs package mgcv (Wood, 2017). (b) Partial residual plot showing the combined influence of fishing effort and slope on rugosity. Contours of rugosity indicate the GAM fit to data for the whole Whittard Canyon region, controlling for the other predictors in the best model. Points indicate the distribution of observations for each predictor. [One column wide]

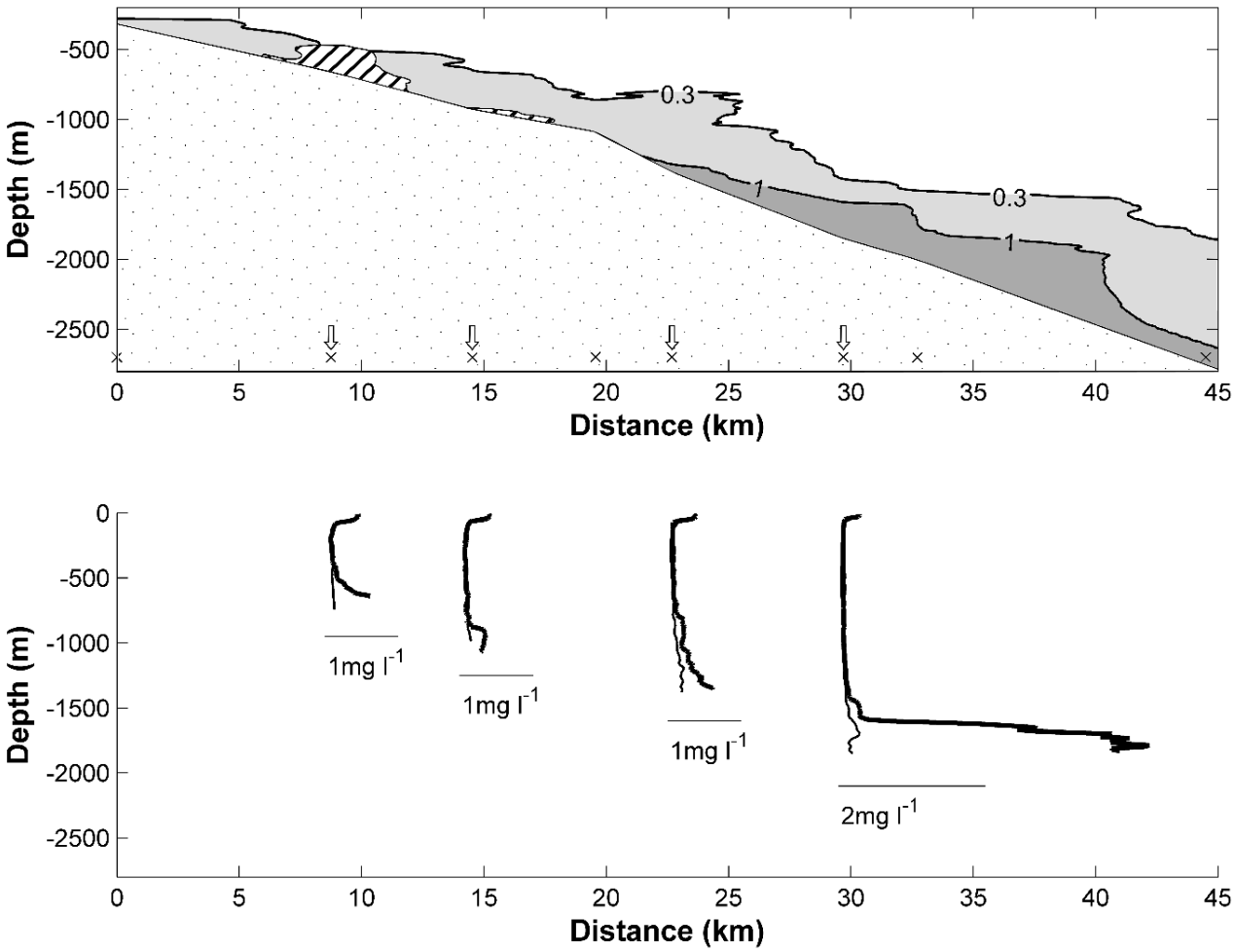

Fig. 7. (a) Along channel section of SPM concentration (mg l^{-1}) in WC4 in the immediate aftermath of a trawling plume, showing the 0.3 and 1 mg l^{-1} contours only. For comparison the hatched area indicates the regions where SPM concentrations > 0.3 mg l^{-1} were measured in other canyon branches when no trawling plumes were evident during the survey. The station locations are shown by the 'x'. In (b), selected vertical profiles of SPM for the above section are indicated in the thick line with thin line showing examples from the same depth in unaffected branches. [1.5 columns wide]

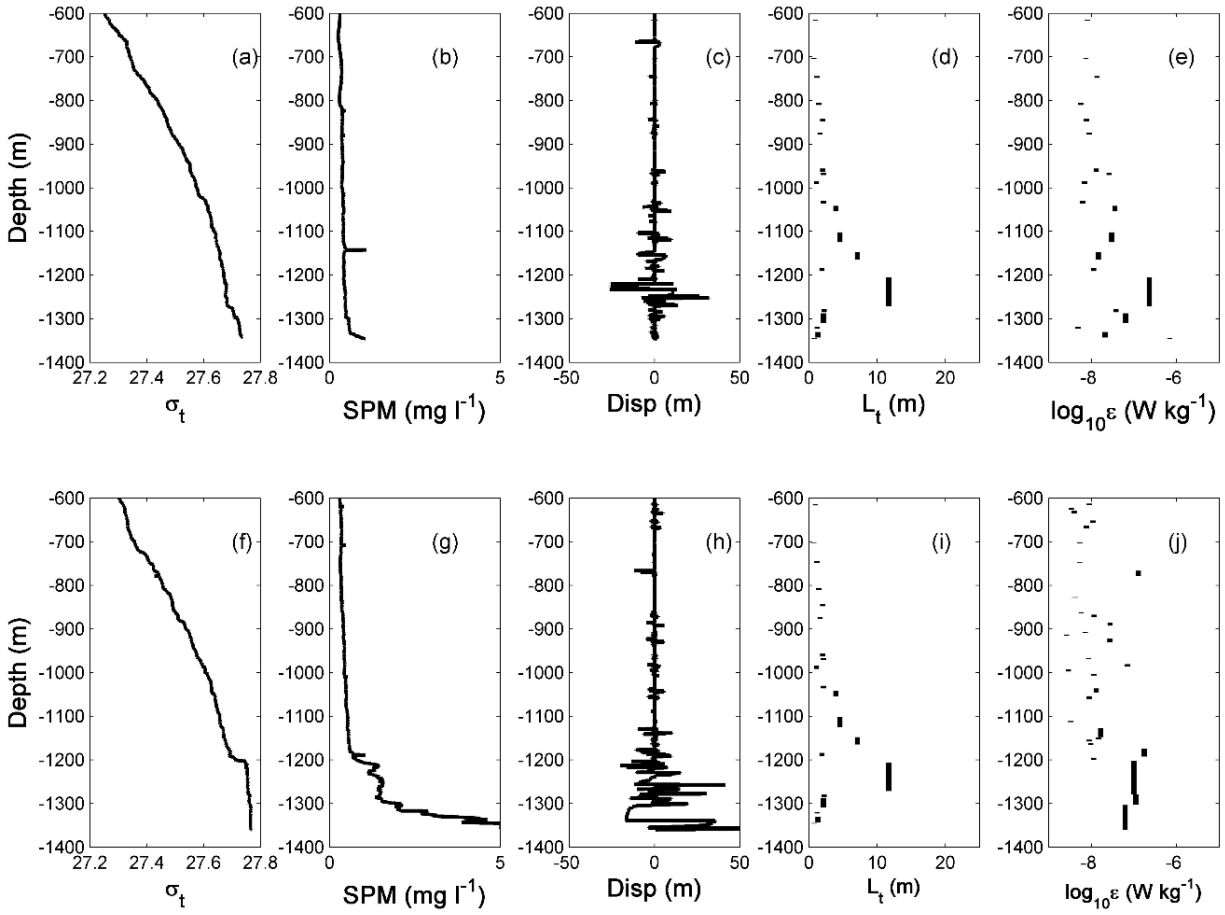

Fig. 8. Vertical profiles of (a) σ_t, (b) SPM (mg l^{-1}), (c) Individual Thorpe displacements (m), (d) Thorpe Length Scale for overturns (m) and (e) $\log_{10}$ of the turbulent energy dissipation (ε, W kg^{-1}), for the WC4 location at ~ 1380 water depth in 2016 (see Fig. 2a; K8). (f-j) are the corresponding profiles at the same location during a plume event 31 hours later. Note in (g), the SPM scale is cut off at 5 mg l^{-1}, for clarity – the maximum value in the near bottom turbid layer was 8 mg l^{-1}. [Two columns wide]

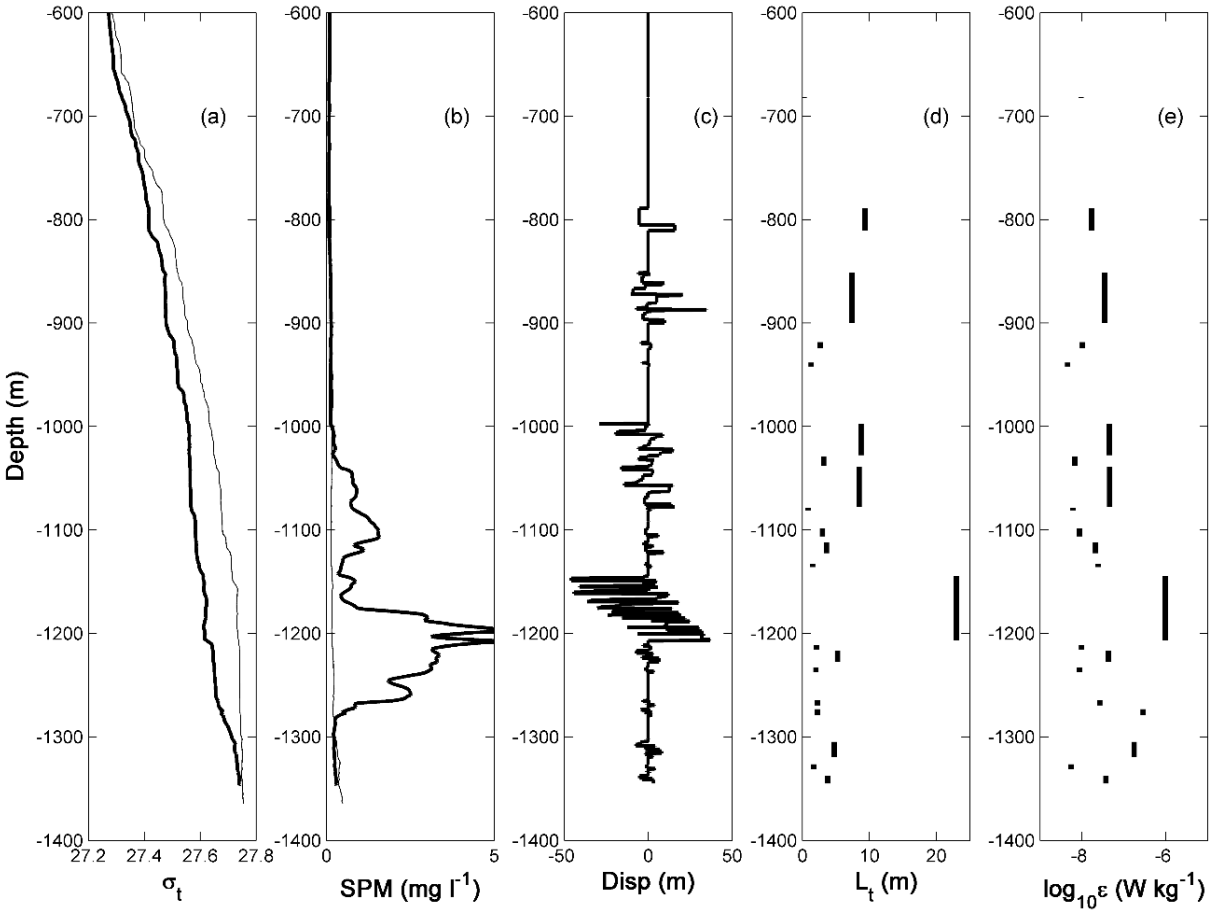

Fig. 9. Vertical profiles of **(a)** σ_t, **(b)** SPM (mg l^{-1}), **(c)** Individual Thorpe displacements (m), **(d)** Thorpe Length Scale for overturns (m) and **(e)** $\log_{10}$ of the turbulent energy dissipation (ε, W kg^{-1}), for the WC3 location at ~ 1385 water depth, 2013 (see Fig. 2a; K9). [Two columns wide]

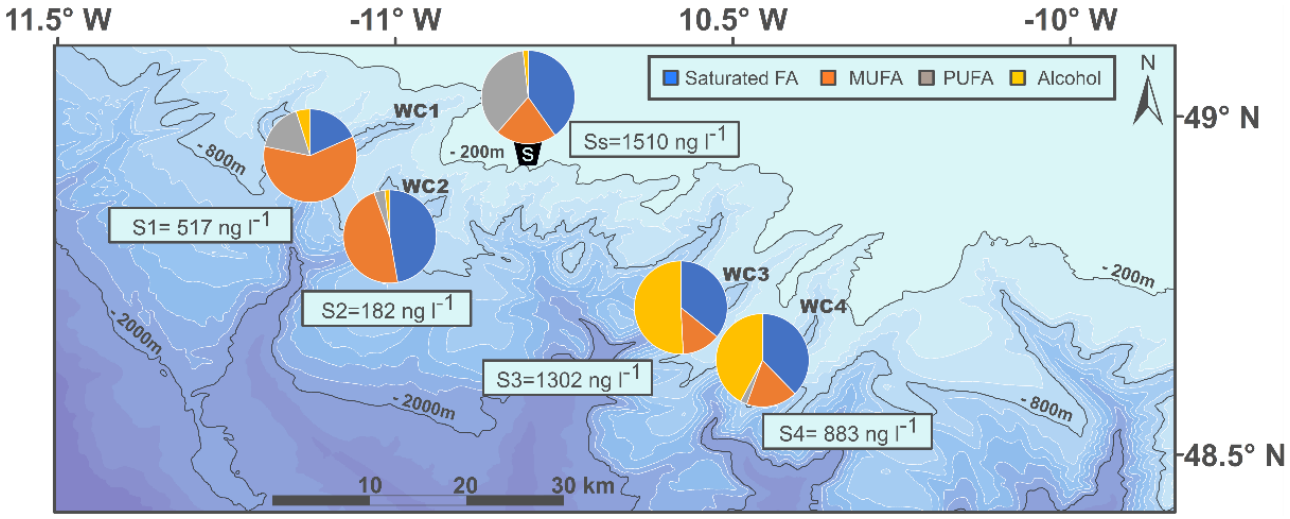

Fig. 10. Map image showing concentrations of total lipids normalised to volume of water (ng l^{-1}) detected in suspended particulate organic matter collected in four branches (WC1 – 4) and at the surface of Whittard Canyon in June 2013. Pie charts show the contribution of saturated fatty acids, monounsaturated fatty acids (MUFAs), polyunsaturated fatty acids (PUFAs) and fatty alcohols in each sample (locations: S1 – 4 and surface sample Ss; see Fig. 2a). [1.5 columns wide]

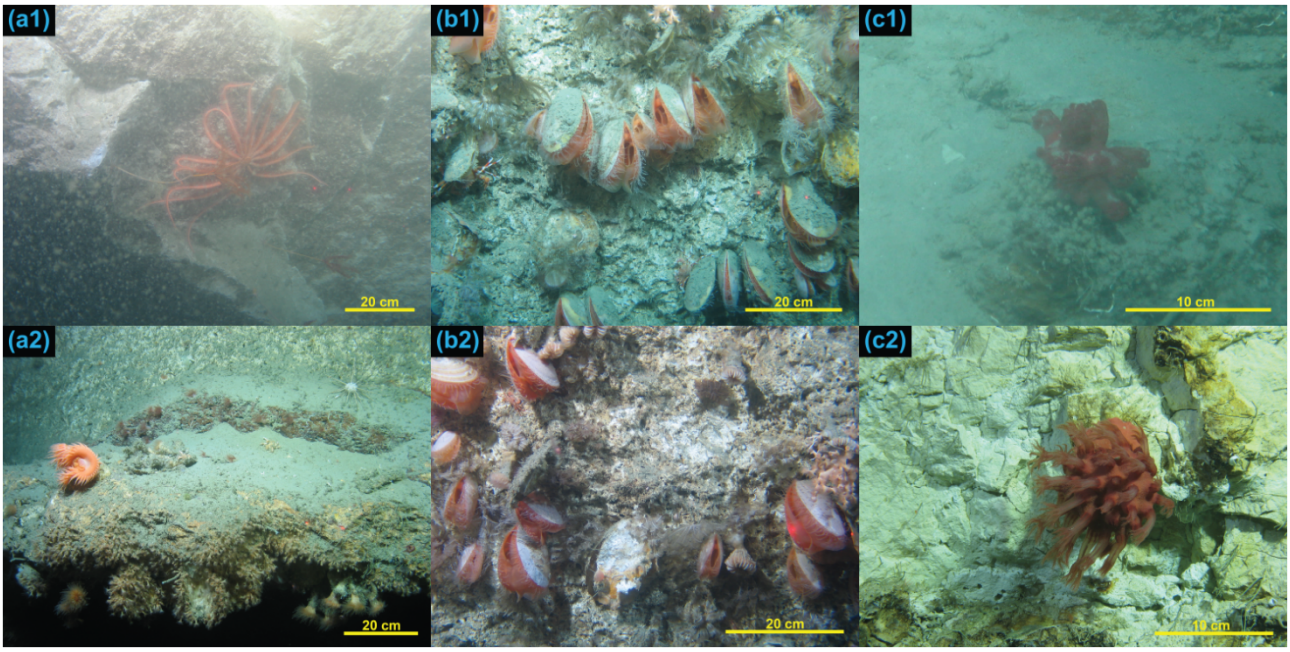

Fig. 11. Photo images from Whittard Canyon 2013 – 2016, displaying contrasting sediment concentrations both in the water column and resettling on benthic fauna. (a1): Cloudy water surrounds a Brisingid starfish; WC3. (a2): Very clear water and a Flytrap anemone; WC1. (b1): Sediment laden *Acesta excavata*; WC3. (b2): Clean *A. excavata*; WC3. (c1): The soft coral Anthomastus topped with a vail of sediment; WC3. (c2): An Anthomastus perched on a canyon wall with polyps fully extended. Note that the Anthomastus (c1) with retracted polyps may have become sediment covered during earlier ROV manoeuvres adjacent to site (visibility was not sufficient to determine this from the video), but the quantity of loose sediment available for such coverage may have been introduced by trawling. [Two columns wide]

Table 1. Generalised Additive Model (GAM) fits to predict rugosity values in the full dataset, excluding cells with zero fishing (n = 6241 grid cells). Model predictors: R = Rugosity, Ln = longitude, Lt = Latitude, V = VMS fishing hours, S = slope angle. Variables in brackets have been modelled as interacting predictors. Generalised Cross Validation (GCV) scores indicate the relative performance of models, with lower values indicating better fits. Adjusted R^2 values are a less robust indicator of model fit, but are included as their interpretation is more intuitive as an indicator of the performance of models at fitting the data.

Model	**Terms**	**GCV x10^{-5}**	**Adj R^2 %**
1	Ln + Lt	6.12	38.9
2	S + V	3.39	64.1
3	Ln + Lt + S + V	2.51	74.9
4	(Ln x Lt x S x V)	2.53	74.9
5	(Ln x Lt) + V	4.81	52.1
6	(Ln x Lt) + (S x V)	2.46	75.6
7	(Ln x Lt) + S	2.49	55.2

Table 2: Fishing intensity (hrs/km2) for each canyon branch, showing results for whole branches and also broken down into specific areas within branch.

	Whole canyon branch			**Shallower and higher fished interfluves**			**Areas directly above 20° slope**		
	Fishing (hours)	Area (Km^2)	Effort (hrs/km^2)	Fishing (hours)	Area (Km^2)	Effort (hrs/km^2)	Fishing (hours)	Area (Km^2)	Effort (hrs/km^2)
WC1	5755.6	220.4	26.1	5264.4	101.0	52.1	54.3	10.0	5.4
WC2	5926.7	264.8	22.4	5766.4	92.1	62.6	133.6	12.0	11.1
WC3	8847.2	214.1	41.3	8423.5	118.1	71.3	196.5	12.4	15.9
WC4	11132.3	260.9	42.7	10779.5	135.5	79.6	278.6	13.1	21.3

Table 3. Biogeochemical data for four samples (Locations S1 – 4; see Fig. 2a) and the surface sample (Ss) used in this study with mean ± standard deviation for Western and Eastern samples. SPM: suspended particulate matter; C:N: molar carbon to nitrogen ratio; MUFA: monounsaturated fatty acids; PUFA: polyunsaturated fatty acids. Individual compounds, lipid group and primary biomarkers used for indices are shown in the Appendix. * indicates torn filters

Variable	**Unit**	**SURFACE**	**WEST**				**EAST**			
Branch		*	WC1*	WC2*			WC3*	WC4		
Sample depth (mab)		12	1308 (12 mab)	1335 (20 mab)	mean	SD	1370 (7mab)	1368 (15mab)	mean	SD
SPM	mg l^{-1}	NA	1.18	0.43	0.80	0.53	0.29	2.16	1.23	1.32
C/N	Molar	6.36	22.19	9.25	15.72	9.15	19.52	8.16	13.84	8.03
Total lipids normalised to water	ng l^{-1}	1510.44	517.07	181.50	349.29	237.29	1301.85	882.74	1092.30	296.36
Saturated fatty acids	ng l^{-1}	607.40	94.96	85.79	90.37	6.48	465.90	332.84	399.37	94.09
MUFA	ng l^{-1}	319.84	309.20	85.66	197.43	158.07	174.37	157.16	165.77	12.17
PUFA	ng l^{-1}	556.22	87.29	6.87	47.08	56.86		20.72	20.72	
Alcohol	ng l^{-1}	26.98	25.63	3.18	14.40	15.87	661.58	372.03	516.80	204.75
Saturated fatty acids	%	40.21	18.36	47.27	32.82	20.44	35.79	37.70	36.75	1.36
MUFA	%	21.18	59.80	47.19	53.50	8.91	13.39	17.80	15.60	3.12
PUFA	%	36.82	16.88	3.79	10.33	9.26	0.00	2.35	1.17	1.66
Alcohol	%	1.79	4.96	1.75	3.35	2.26	50.82	42.14	46.48	6.13
Unsaturated fatty acids	%	58.00	76.68	50.98	63.83	18.17	13.39	20.15	16.77	4.78
INDICES										
Phyto	ng l^{-1}	1182.73	315.85	136.39	226.12	126.90	1222.93	820.26	1021.59	284.73
	%	78.30	61.09	75.15	68.12	9.94	93.94	92.92	93.43	0.72
	ng l^{-1}	66.85	25.92	13.93	19.93	8.47	20.50	29.83	25.17	6.60
Bacterial	%	4.43	5.01	7.68	6.35	1.88	1.57	3.38	2.48	1.28

Appendix [supplementary data]

List of compounds most commonly identified in this study with groups and their corresponding IUPAC names. Individual compounds used for the phytoplankton and bacterial indices are indicated.

Compound	Group	IUPAC name	Reference for lipid biomarker/indices
br-C14:1	MUFA	Tetradecanoic acid (double bond position unknown)	
C14:1 (n-5)	MUFA	9-Tetradecenoic acid	
C14:0 acid	SFA	Tetradecanoic acid	Phytoplankton (Conte et al. 2003; Harwood and Russell, 1984)
C14:0 alcohol	Alcohol	Tetradecan-1-ol	Phytoplankton (Volkman et al., 1998)
C15:1(n-5)	MUFA	Methyl 10-cis-pentadecenoate	Bacteria (Volkman & Johns, 1977; Duineveld et al., 2012)
i-C15:0	BFA	12-Methyltetradecanoic acid	Bacteria (Volkman & Johns, 1977; Duineveld et al., 2012)
a-C15:0	BFA	12-Methyltetradecanoic acid	Bacteria (Volkman & Johns, 1977; Duineveld et al., 2012)
C15:0	SFA	Pentadecanoic acid	Phytoplankton (Conte et al. 2003; Harwood and Russell, 1984); Bacteria (Volkman & Johns, 1977; Duineveld et al., 2012)
br-C16:1	MUFA	Hexadecenoic acid (double bond position unknown)	
C16:1(n-7)	MUFA	9-Hexadecenoic acid	Phytoplankton (Conte et al. 2003; Harwood and Russell, 1984)
C16:0 acid	SFA	Hexadecanoic acid	Phytoplankton (Conte et al. 2003; Harwood and Russell, 1984)
C16:0 alcohol	Alcohol	1-Hexadecanol	Phytoplankton (Volkman et al., 1998)
br/st-C17:1	MUFA	Heptadecenoic acid double bond position unknown)	Bacteria (Volkman & Johns, 1977; Duineveld et al., 2012)
C17:0 acid	SFA	Heptadecanoic acid	Phytoplankton (Conte et al. 2003; Harwood and Russell, 1984); Bacteria (Volkman & Johns, 1977; Duineveld et al., 2012)
C18:3(n-6)	PUFA		Phytoplankton (Duineveld et al. 2012)

C18:2(n-6)	PUFA		Phytoplankton (Duineveld et al. 2012)
C18:1(n-9)	MUFA		
C18:1(n-7)	6,9,12-Octadecatrienoic acid		Bacteria (Volkman & Johns, 1977; Duineveld et al., 2012)
C18:0 acid	9,12-Octadecadienoic acid		Phytoplankton (Conte et al. 2003; Harwood and Russell, 1984)
C18:0 alcohol	9-Octadecenoic acid		Phytoplankton (Volkman et al., 1998)
C20:5(n-3)	11-Octadecenoic acid		Phytoplankton (Duineveld et al. 2012)
C20:3	Octadecanoic acid	Eicosadienoic acid (double bond position unknown)	Phytoplankton (Duineveld et al. 2012)
C20:2	1-Octadecanol	Eicosadienoic acid (double bond position unknown)	Phytoplankton (Duineveld et al. 2012)
C20:1(n-9)	5,8,11,14,17-Eicosapentaenoic acid	11-Eicosenoic acid	
C20:0 acid	SFA	Eicosanoic acid	Phytoplankton (Conte et al. 2003; Harwood and Russell, 1984)
C20:0 alcohol	Alcohol	1-Eicosanol	Phytoplankton (Volkman et al., 1998)
C21:0 acid	SFA	Heneicosanoic acid	Phytoplankton (Conte et al. 2003; Harwood and Russell, 1984)
C22:6 (n-3)	PUFA	Docosahexaenoic acid	Phytoplankton (Duineveld et al. 2012)
C22:1(n-9)	MUFA	Tetracos-15-enoic acid	
C22:0 acid	SFA	Docosanoic acid	Phytoplankton (Conte et al. 2003; Harwood and Russell, 1984)
C24:1 (n-9)	MUFA	Nervonic	